

**Probing the Active Site of Amine Oxidase  
with Electron Tunneling Wires**

**Thesis by  
Corinna R. Hess**

**In Partial Fulfillment of the Requirements  
for the Degree of  
Doctor of Philosophy**

**California Institute of Technology  
Pasadena, California**

**2002**

**(Defended May 30, 2002)**

© 2002

Corinna R. Hess

All Rights Reserved

## Acknowledgments

Six years seems like a very long time, at least right now, and two pages much too short, but here goes...

There are many people to whom I am very grateful for all their help on this project and for all that they have taught me. Dave Dooley gave me the chance to work on this project and has shown great patience despite all the detours we've taken it on. His group, especially Greg Juda, has sent protein at a moments notice and provided many helpful discussions as well. I've been lucky to have worked with Mike Hill on this project. He has taught me a lot about this "black box" of protein e-chem, and was thankfully always optimistic even when things looked somewhat bleak. The project has also been pushed forward these past few months by the talent and tenacity of a student of his, Ricky Amii. I owe a million thanks to Michele McGuirl, who was enormously helpful in my initial venture into the bio world. She taught me the bulk of what I know about amine oxidase and most importantly has always believed in this project. It seems fitting that my undergraduate advisor, Greg Hillhouse, be here at Caltech as I finish up. I have him to thank for introducing me to research. I wouldn't be here if it weren't for the great experience of the 3 and ½ years I spent in his lab and for his continuing support.

The Gray group has always been made up of many unique personalities who've made the experience of grad school enjoyable, and sometimes very entertaining. I'm very fortunate to have met and worked with many wonderful people; Randy, Mike, Akif, Cissi, have all been great not only to discuss science with, but I've also shared many memorable moments with them and they've been there for periods of high stress as well.

The heart and soul of the Gray group are of course Harry and Jay. I've learned a great deal from Jay and his patience is truly impressive. We've definitely abused his open-door policy. But no matter how busy, I could always plop down on his couch with a look of confusion, and he would take the time to discuss my project with me. He always had a plan B available when things looked grim (actually, I think we've exhausted the first half of the alphabet). And Harry, I couldn't have asked for a better advisor. He always knew when I needed encouragement, when I needed a kick in the ..., and when it had been a particularly frustrating week and I just needed a shot of whiskey. I am extremely grateful to him for his confidence in this project, his motivation, and for not letting me give up.

All of the ups and downs of these past six years have been shared by my best friends. My appreciation for their friendship cannot be expressed enough. Jenn has been to Brussels and back with me (twice). I'm going to miss all of our adventures (not so much those spring rolls) though I'm sure there are still many ahead. Her sense of humor has always made me laugh, and her generosity is amazing. Natia has also always been there for me and her friendship has been invaluable. Our hour-long discussions about chemistry, life, love, politics, etc. have kept me sane. She has an amazing insight into everything and always had good advice and loads of encouragement.

Finally, I have my family to thank for their unwavering support in all of my efforts. My parents have always encouraged and believed in me. They have celebrated every accomplishment, no matter how small. My brother has always commiserated with me and I've been very lucky to have my sister out here these past two years. Their support has meant a lot to me.



## Abstract

Amine oxidases (AO) are copper-containing enzymes that catalyze the conversion of amines to aldehydes. The active site is deeply buried within the protein network, a factor which has precluded many investigations into the mechanism. A series of electron tunneling molecular wires has been synthesized, designed to access the cofactors of amine oxidase by means of the substrate channel. These wires are comprised of phenyl-ethynyl units and thus promote rapid rates of electron transfer to the active site. An amine group attached to one end of the oligomer serves as the channel-specific functionality, which binds within the channel. Binding of the oligomers to AO was demonstrated through inhibition and fluorescence quenching studies. A variety of reporter groups has been attached to the chain end opposite the amine group, allowing us to probe the enzyme using a variety of techniques. A Re terminated complex was designed for electron transfer studies with the enzyme. The photophysics of this complex were investigated in the presence of AO. A thiol terminated wire also has been synthesized, which was employed in electrochemical studies of the amine oxidase cofactors. These studies provide evidence for the ability to communicate with the active site using the molecular wires. In addition, these complexes fulfilled our primary goal and enabled us to determine a redox potential of the TPQ cofactor.

## Table of Contents

Acknowledgment .....	iii
Abstract .....	v
Table of Contents .....	vi
List of Figures and Tables .....	ix
Chapter 1: Introduction .....	1
Amine oxidase background .....	2
Thesis overview and objectives .....	8
References .....	11
Chapter 2: Electrochemistry of amine oxidases .....	12
Materials and methods .....	17
Electrochemistry .....	18
Electrode preparations .....	18
Results .....	19
Discussion .....	23
References .....	26
Chapter 3: Design and synthesis of molecular wires for amine oxidases .....	27
Inhibition studies .....	29
Materials and methods .....	29
Results .....	32
Synthesis of molecular wires .....	32
References .....	37
Chapter 4: Binding of molecular wires to AGAO .....	38

Materials and methods -----	40
Results and discussion -----	42
Chapter 5: Photochemical investigations of Re(BzA-1-DEA) with AGAO -----	47
Modeling of Re(BzA-1-DEA) into the AGAO channel -----	49
Materials and methods -----	51
Results -----	51
Discussion -----	54
Photophysics of Re(BzA-1-DEA) -----	54
Photophysics of Re(BzA-1-DEA) with AGAO -----	61
References -----	63
Chapter 6: Electrochemistry of AGAO with DEA-1-PhSH -----	64
Materials and methods -----	67
Electrochemistry -----	68
Electrode preparations -----	68
Modifications of Au electrodes with thiol wires -----	69
Determination of thiol coverage on Au electrodes -----	69
Electrochemistry of DEA-1-PhSAc -----	69
Results -----	69
Discussion -----	70
Electrochemistry of DEA-1-PhSH -----	72
Results -----	72
Discussion -----	76
References -----	78

Appendix A: Protein purification and sample preparation .....	79
Protein expression and purification .....	80
AGAO sample preparation .....	80
References .....	81
Appendix B: Synthesis and characterization of molecular wires .....	82
General .....	83
General procedures for Pd cross-coupling reactions .....	83
Synthesis and purification of oligomers .....	86
Synthesis of Re(BzA-1-DEA) .....	94
References .....	97

## List of Figures and Tables

### Chapter 1

Figure 1.1: Crystal structure of AGAO -----	3
Figure 1.2: Proposed mechanism for TPQ biogenesis -----	6
Figure 1.3: Catalytic cycle of amine oxidase -----	7

### Chapter 2

Figure 2.1: Depiction of electrode surfaces for protein electrochemistry -----	14
Figure 2.2: Residues comprising the channel of AGAO -----	16
Figure 2.3: SWV of AGAO on PGE electrodes -----	20
Figure 2.4: SWV of AGAO on (KC) <sub>2</sub> modified Au electrodes -----	21
Figure 2.5: SWV of AGAO on (KC) <sub>2</sub> modified Au electrodes -----	22

### Chapter 3

Table 3.1: Molecules used for inhibition studies of AGAO -----	30
Figure 3.1: Results of inhibition studies of AGAO -----	33
Figure 3.2: Methodology for synthesis of wires -----	34
Figure 3.3: Wires synthesized for communication with the active site AO -----	36

### Chapter 4

Figure 4.1: Absorption and emission spectra of DEA-1-BzA -----	41
Figure 4.2: Time-resolved fluorescence quenching of DEA-1-BzA by AGAO	43
Figure 4.3: Steady-state fluorescence quenching of DEA-1-BzA by AGAO --	44
Figure 4.4: Results of inhibition studies of AGAO with DEA-1-BzA -----	46



## Chapter 5

Figure 5.1: Model of Re(BzA-1-DEA) in the AGAO channel -----	50
Figure 5.2: Absorption spectrum of Re(BzA-1-DEA) -----	52
Figure 5.3: Emission spectra of Re(BzA-1-DEA) -----	53
Figure 5.4: Transient absorption spectrum of Re(BzA-1-DEA) in dioxane -----	55
Figure 5.5: Transient absorption spectra of Re(BzA-1-DEA) -----	56
Figure 5.6: Log lot of transient absorption spectra -----	57
Figure 5.7: Transient absorption spectra of Re(BzA-1-DEA) -----	58
Figure 5.8: Diagram for the excited states of Re(BzA-1-DEA) -----	60

## Chapter 6

Figure 6.1: Depiction of self-assembled protein monolayers on gold -----	66
Figure 6.2: Electrochemistry of AGAO with DEA-1-PhSAc -----	71
Figure 6.3: CV of AGAO on electrodes modified with DEA-1-PhSH/AGAO --	73
Figure 6.4: OSWV of AGAO on DEA-1-PhSH modified Au electrodes -----	74
Figure 6.5: Difference spectrum for OSWV on DEA-1-PhSH modified Au ----	75

## Appendix B

Figure B.1: Synthesis scheme for molecular wire precursors -----	84
Figure B.2: Scheme for synthesis of molecular wires -----	85
Figure B.3: $^1\text{H}$ NMR of <b>iii</b> in $\text{CDCl}_3$ -----	87
Figure B.4: $^1\text{H}$ NMR of <b>vi</b> in $\text{dmf-d}_6$ -----	89
Figure B.5: $^1\text{H}$ NMR of <b>DEA-1-BzA</b> in $\text{dmf-d}_6$ -----	90
Figure B.6: $^1\text{H}$ NMR of <b>DEA-1-PhSAc</b> in $\text{CD}_2\text{Cl}_2$ -----	92
Figure B.7: $^1\text{H}$ NMR of <b>DEA-1-PhSAc</b> in $\text{CD}_2\text{Cl}_2$ -----	93



Figure **B.8**:  $^1\text{H}$  NMR of **Re(BzA-1-DEA)** in  $\text{CD}_3\text{CN}$  ----- 95

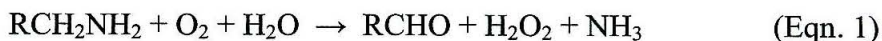
Figure **B.9**:  $^1\text{H}$  NMR of  $(\text{phen})\text{Re}^{\text{I}}(\text{CO})_3(\text{OH}_2)]^{\text{Tf-}}$  in  $\text{dmf-d}_6$  ----- 96

## **Chapter 1**

### **Introduction**

### *Amine Oxidase Background*

Copper amine oxidases are enzymes that catalyze the conversion of primary amines to aldehydes (Equation 1).



Amine oxidases (AOs) are found in virtually all organisms. They have been isolated from bacteria, yeast, fungi, plants and animals. The enzymes encompass a broad range of substrate specificity and serve a diversity of functions in each organism<sup>1,2</sup>. In bacteria and yeast, amine oxidase permits growth on amines as the sole source of nitrogen and carbon. In plants, the enzymes are involved in cell wall and lignin formation processes associated with wound healing. They also have been shown to play a role in cell growth through regulation of biogenic amines. The role of amine oxidases in mammals is less well understood. They are believed to be crucial for the regulation of biogenic amines. It has been suggested that the enzymes play a role in cell regulation and cellular signaling processes due to H<sub>2</sub>O<sub>2</sub> production upon reaction with amines.

Amine oxidase is a homodimer with subunits of molecular mass in the range of 70–95 kDa. Each subunit contains one copper site and one organic cofactor. Crystal structures have been solved for bacterial AOs (*E. coli*; ECAO and *Arthrobacter globiformis*; AGAO)<sup>3,4</sup>, yeast AO (*Hansenula polymorpha*; HPAO)<sup>5</sup> and plant AO (pea seedling; PSAO)<sup>6</sup>. (To date, a mammalian AO has not been crystallized.) There are general features common to all amine oxidases. The two subunits together form a mushroom-cap shaped structure (shown in Figure 1.1 for AGAO). Each subunit consists of three domains. Domain 4 is the largest of these and comprises the region for

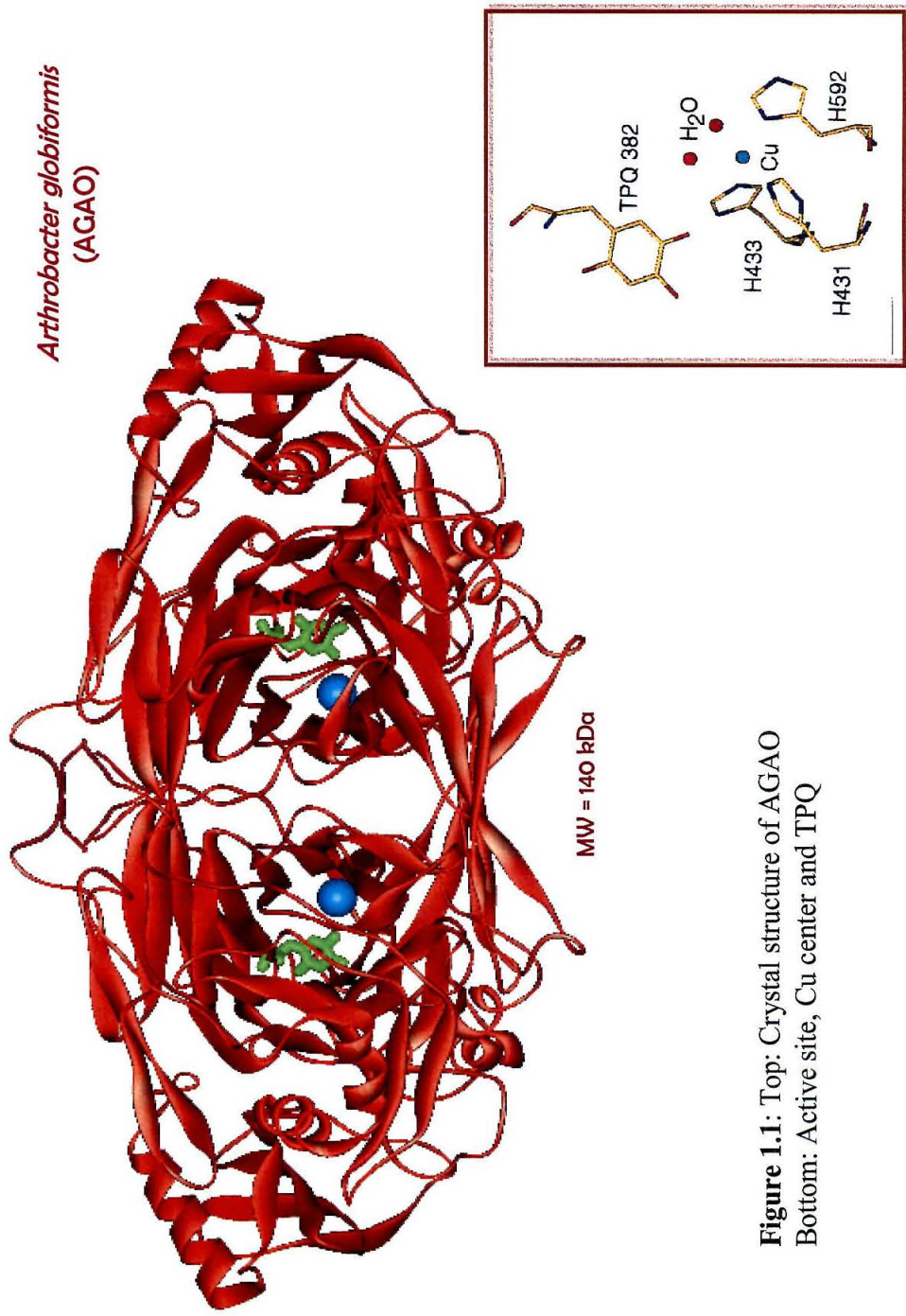


**Figure 1.1:** Top: Crystal structure of AGAO  
Bottom: Active site, Cu center and TPQ

intersubunit contact. Domains 2 and 3 are located at the periphery of the enzyme, on the surface of D4. There are two  $\beta$  hairpin arms that extend from D4 of each subunit and wrap around the second subunit. Arm II lies along the surface at the top of the molecule, whereas Arm I is located near the bottom and extends into the protein network. Arm I has been suggested to play a role in intersubunit cooperativity. The crystal structures also revealed the presence of a solvent filled channel leading from the protein surface to the active site. This channel is thought to provide the pathway by which substrates access the AO cofactors. The overall volume of the channel varies among AOs, but is  $\sim 20$  Å deep in most cases. Interestingly, this channel is not present in the structure of ECAO.

The active site of amine oxidase consists of a copper center and a topaquinone cofactor (TPQ) (Figure 1.1). The copper center is ligated by three histidines and two water molecules in a square pyramidal geometry, and in the resting state of the enzyme contains Cu(II). The nature of the organic cofactor in amine oxidase was not resolved until 1990. Studies by Klinman and coworkers conclusively identified this molecule as the quinone form of 2,4,6-trihydroxyphenylalanine, using labeling studies in combination with mass spectral and NMR techniques<sup>7</sup>. The cofactor was subsequently characterized by resonance Raman as well<sup>8</sup>. The topaquinone is generated by post-translational modification of a tyrosine residue in the precursor protein. This process does not require the presence of chaperones or external cofactors. The precursor enzyme utilizes only molecular oxygen and the protein bound Cu in this reaction. The mechanism for TPQ biogenesis has received considerable attention but is still poorly understood. Of particular interest is the role of the copper center in the six-electron



oxidation of tyrosine, since Cu traditionally acts as a  $1e^-$  oxidant. Based on numerous investigations, a mechanism has been proposed for TPQ biogenesis (Figure 1.2)<sup>9</sup>. Tyrosine is believed to initially bind to the Cu site, which then activates the residue for reaction with  $O_2$ . This activated intermediate is believed to be either a one-electron oxidized  $Cu^I\text{-Tyr}^\bullet$  complex or one in which charge is delocalized over a  $Cu^{II}\text{-Tyr}^-$  unit, rendering the tyrosine more susceptible to attack by  $O_2$ . Formation of this intermediate is believed to be the rate-determining step in the overall reaction. Support for the remaining steps was obtained from resonance Raman and computational studies. However, none of the postulated intermediates has been directly observed. The degree to which the copper participates in the redox chemistry of the enzyme has yet to be ascertained. The copper site may play primarily a structural role or serve to stabilize the various intermediates. It is uncertain whether the metal itself undergoes a formal change in oxidation state in any of these steps. Copper is required for TPQ biogenesis, nonetheless. Substitution of other metal ions in precursor AO does not result in cofactor formation.

The reaction mechanism of AOs with amines has also been studied extensively and many of the intermediates have been spectroscopically characterized<sup>2,10</sup>. The catalytic cycle is shown in Figure 1.3. In the reductive half-reaction, topaquinone undergoes attack at the C-5 position by the primary amine to initially generate a substrate Schiff base intermediate. This Schiff base complex undergoes proton abstraction by a nearby Asp residue. Subsequent hydrolysis releases the product aldehyde and generates the  $2e^-$  reduced aminoquinol ( $TPQ_{RED}$ ). Dioxygen reacts with the aminoquinol in the oxidative half-reaction, producing  $H_2O_2$ ,  $NH_3$  and the oxidized form



Taken from: McGuirl, M.A., Dooley, D.M *Curr. Op. Chem. Biol.* **1999**, 3, 138-144.

### Amine Oxidase Mechanism

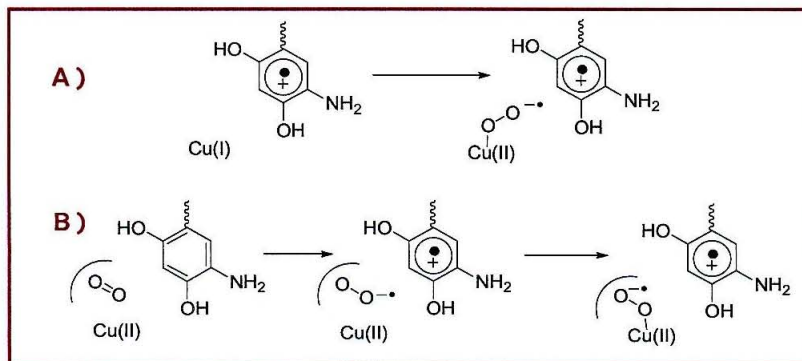
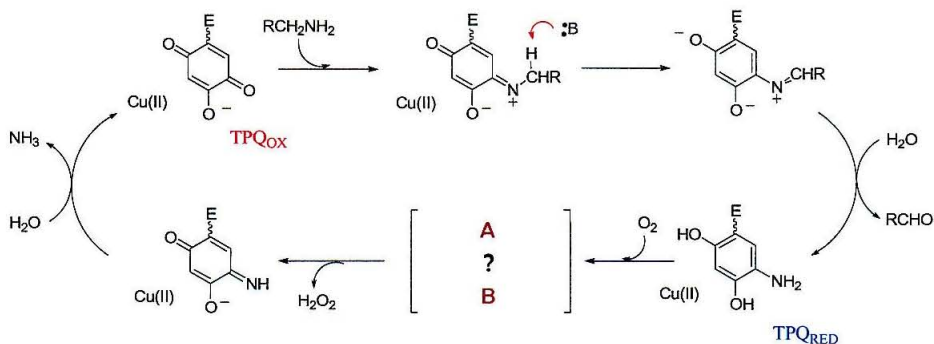


**Figure 1.3:** Top: Catalytic cycle of amine oxidase  
 Bottom: Proposed intermediates for the oxidative half-reaction;  
 (A)  $\text{Cu}^{\text{I}}$ -SQ intermediate, (B) alternative mechanism with  $\text{O}_2$  binding pocket.

of the cofactor (TPQ<sub>ox</sub>).

The mechanism for the oxidative half-reaction has been the subject of considerable debate as well, particularly in regard to the role of the copper center. Dooley and coworkers obtained EPR evidence for a Cu<sup>I</sup>-semiquinone (Cu<sup>I</sup>-SQ) intermediate (Figure 1.3a), which indicated that Cu was actively involved in the regeneration of TPQ<sub>ox</sub><sup>11</sup>. According to their mechanism, the aminoquinol transfers one electron to the copper site to generate Cu<sup>I</sup>-SQ. Dioxygen binds Cu(I) and is reduced by one electron to generate a Cu<sup>II</sup>-O<sub>2</sub><sup>•-</sup> intermediate, and the second electron is obtained from the semiquinone. Arguments against Cu<sup>I</sup> involvement suggest that formation of the Cu<sup>I</sup>-SQ species is off pathway. Evidence for prebinding of dioxygen to a hydrophobic pocket in the enzyme, not at the copper site, supports this interpretation<sup>12</sup>. Recent studies in the Klinman lab have demonstrated that the Co(II) substituted enzyme is also catalytically active at a rate comparable to that of the native enzyme<sup>13</sup>, confirming that copper is not necessary for enzyme activity. The metal may instead play a structural role or serve to stabilize a superoxide intermediate (Figure 1.3b).

### *Thesis Overview and Objectives*

Our objective was to address some of the mechanistic issues through electrochemical and electron transfer studies of amine oxidase. Prior to our work, the potentials of the amine oxidase cofactors had not been measured. Studies using model complexes of topaquinone indicate that this potential should be ~ -200 mV vs. SCE<sup>14</sup>. The protein environment, particularly the interaction with the copper site, and substrate binding are expected to alter the potential of the cofactor compared to the value in

solution. Accurate determination of these values could provide information concerning the mechanisms for the conversion of amines as well as the biogenesis of TPQ. A measurement of the  $\text{Cu}^{\text{II/I}}$  potential and comparison with the aminoquinol potential would shed some light on the nature of the redox equilibrium between the cofactors. Since a  $\text{Cu}^{\text{I}}$ -SQ species has been implicated as a key intermediate in the catalytic cycle, knowing the  $\text{Cu}^{\text{II/I}}$  potential could provide evidence in favor of this mechanism. A Cu(I) intermediate has also been suggested in the initial activation of the Tyr in the precursor enzyme. The potential for oxidation of a metal-bound tyrosine can be estimated as  $\sim 500$  mV vs. NHE. The potential of the copper complex must therefore be greater than this value to generate the tyrosine radical and, if it is in this range, the copper could easily oxidize the aminoquinol as well. It is of interest to compare the potentials of the copper site in the precursor enzyme to that of the fully processed AO.

We have pursued electron transfer studies on amine oxidase in the hope of detecting some of the intermediates throughout TPQ biogenesis. The oxidation of tyrosine is the rate-determining step in the overall mechanism. By performing this initial slow step using an external oxidant in combination with ultrafast spectroscopy, we could potentially detect some of the subsequent intermediates. Substitution of the Cu with Zn or Ni would then allow us to ascertain the role of the copper in the mechanism.

One of the major challenges in the investigations of amine oxidases is communicating with the active site, as it is deeply buried within the protein. To meet this challenge, we have employed “molecular wires” designed to access the active site of the enzyme by way of the  $\sim 20$  Å substrate channel. This approach has been used previously in the Gray group to study the mechanisms of cytochrome P450<sup>15</sup>. Ru-terminated,



substrate-linked hydrocarbon chains were used to deliver electrons to the heme site of P450. The intermediates generated by this method could then be detected using ultrafast spectroscopy. Crystal structure studies demonstrated that the substrate-tethered Ru complexes bind tightly in the P450 channel<sup>16</sup>.

We have designed oligomers, i.e., “wires”, consisting of phenyl-ethynyl bridging units to permit rapid electron transfer to and from the AO active site. These complexes are terminated on one end with amine substituents designed to mimic the natural substrates and bind within the enzyme channel. The nature of the second functional group was varied to permit studies of the enzyme by photophysical and photochemical techniques. Thiol terminated oligomers, which were synthesized for the purpose of electrochemical studies, are the subject of Chapter 5. Metal-terminated complexes for photophysics and photochemistry are treated in Chapter 6. The complexes are all highly fluorescent, such that binding of the oligomers to the enzyme was determined through variations in emission intensities and lifetimes.

The studies described above were carried out primarily on amine oxidase from *Arthrobacter globiformis*. The crystal structure of AGAO is known, and the substrate channel is well defined. The oligomers were designed in accordance with the composition and structure of the AGAO channel. The synthesis of these complexes and the results of binding studies as well as electrochemical and photophysical investigations with AGAO are presented in the following chapters.

## References

- (1) Klinman, J. P.; Mu, D. *Annu. Rev. Biochem.* **1994**, *63*, 299-344.
- (2) Halcrow, M.; Phillips, S.; Knowles, P. In *Enzyme-catalyzed electron transfer and radical transfer*; Holzenberg, Scrutton, Eds.; Plenum Publishers: New York, 2000; Vol. 35, pp 183-231.
- (3) Parsons, M. R.; Convery, M. A.; Wilmot, C. M.; Yadav, K. D. S.; Blakeley, V.; Corner, A. S.; Phillips, S. E. V.; McPherson, M. J.; Knowles, P. F. *Structure* **1995**, *3*, 1171-1184.
- (4) Wilce, C. J.; Dooley, D. M.; Freeman, H. C.; Guss, J. M.; Matsunami, H.; McIntire, W. S.; Ruggiero, C. E.; Tanizawa, K.; Yamaguchi, H. *Biochemistry* **1997**, *36*, 16116-16133.
- (5) Li, R. B.; Klinman, J. P.; Mathews, F. S. *Structure* **1998**, *6*, 293-307.
- (6) Vigneich, V.; Dooley, D. M.; Guss, J. M.; Harvey, I.; McGuirl, M. A.; Freeman, H. C. *J. Mol. Biol.* **1993**, *229*, 243-245.
- (7) Janes, S. M.; Mu, D.; Wemmer, D.; Smith, A. J.; Kaur, S.; Maltby, D.; Burlingame, A. L.; Klinman, J. P. *Science* **1990**, 981-987.
- (8) Brown, D. E.; McGuirl, M. A.; Dooley, D. M.; Janes, S. M.; Mu, D.; Klinman, J. *P. J. Biol. Chem.* **1991**, *266*, 4049-4051.
- (9) Dooley, D. M. *J. Biol. Inorg. Chem.* **1999**, *4*, 1-11.
- (10) Klinman, J. P. *Chem. Rev.* **1996**, *96*, 2553.
- (11) Dooley, D. M.; McGuirl, M. A.; Brown, D. E.; Turowski, P. N.; McIntire, W. S.; Knowles, P. F. *Nature* **1991**, *349*, 262-264.
- (12) Su, Q.; Klinman, J. P. *Biochemistry* **1998**, *37*, 12513-12525.
- (13) Mills, S. A.; Klinman, J. P. *J. Am. Chem. Soc.* **2000**, *122*, 9897-9904.
- (14) Mure, M.; Klinman, J. P. *J. Am. Chem. Soc.* **1993**, *115*, 7117-7127.
- (15) Wilker, J. J.; Dmochowski, I. J.; Dawson, J. H.; Winkler, J. R.; Gray, H. B. *Angew. Chem. Int. Ed.* **1999**, *38*, 90-92.
- (16) Dunn, A. R.; Dmochowski, I. J.; Bilwes, A. M.; Gray, H. B.; Crane, B. R. *Proc. Natl. Acad. Sci.* **2001**, *98*, 12420-12425.



## **Chapter 2**

### **Electrochemistry of amine oxidases**

Many difficulties associated with the electrochemistry of proteins are not encountered with small molecules. Proteins have comparatively slow rates of diffusion to the electrode surface, resulting in diminished currents. The surface characteristics of a bare metal electrode do not afford favorable interactions with the surface environment of a protein. Only a few orientations of a protein may permit electron transfer to the active site. Yet these may not be sites of preferred contact with the electrode surface. Adsorption phenomena, leading to conformational changes and protein denaturation, tend to be a common problem as well. These obstacles are generally more prominent for enzymes, which usually are larger and often have deeply buried active sites. Several techniques have been developed to circumvent these problems<sup>1,2</sup>. These methods rely on materials that can provide favorable surfaces for protein-electrode interactions and can be manipulated to accommodate the specific characteristics of a protein. Pyrolytic graphite and modified gold electrodes are two materials that have been successfully employed in the electrochemical investigations of proteins.

Pyrolytic graphite has a crystalline structure much like that of an ideal graphite crystal. This material can be cleaved to generate electrodes of two distinct surface types. Cleavage along the basal plane generates a hydrophobic surface, whereas the edge plane consists of a surface containing various C-O functionalities (such as carboxyl groups). Edge-plane graphite (PGE) electrodes are most commonly used for protein studies. The charged carboxyl groups can participate in electrostatic interactions with residues on the exterior of a protein (Figure 2.1a). If the protein to be studied contains negatively

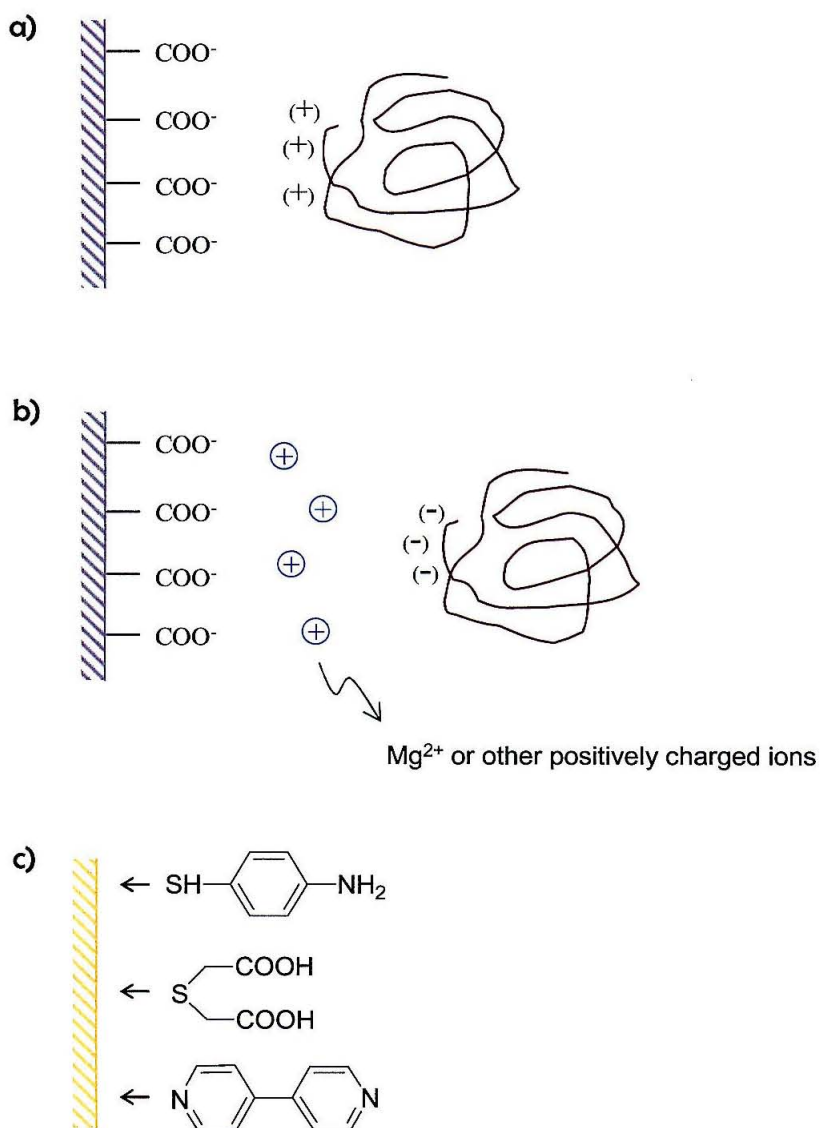


**Figure 2.1:** Electrostatic interactions between PGE electrodes and a) positively charged protein surfaces and b) negatively charged protein surfaces. The latter requires the addition of cations to the solution. c) Commonly used compounds for the modification of gold electrodes.

charged residues at the surface,  $\text{Mg}^{2+}$ ,  $\text{Cr}^{3+}$  or other cations can be added to the solution. This creates a double layer of charge at the PGE-protein interface (Figure **2.1b**).

Gold electrodes can be modified with promoter complexes to create a suitable surface for protein contact<sup>3</sup>. These promoters consist of an X~Y motif. One end of the complex contains the functional group X, which binds to the gold electrode. Thiols, phosphines and pyridyl containing compounds are commonly used with sulfur binding most strongly. The opposing end contains a functional group that interacts with the protein (Y). This group can be varied depending on the properties of the protein to be studied. For example, amino groups can be used for negatively charged proteins, whereas carboxyl containing promoters will favor positively charged proteins. If the active site surroundings are hydrophobic, then the promoter can be designed accordingly. The nature of the linker (~) is variable, but must be oriented in a direction away from the electrode surface.

We have used both PGE and modified gold electrodes for electrochemical studies on amine oxidases. We have investigated the redox properties of AOs from *Arthrobacter globiformis* and bovine plasma. The proteins are negatively charged overall, with pI's of ~ 5 for both AGAO and BPAO. More importantly, the crystal structure of AGAO shows a high concentration of negatively charged residues at the surface of the channel leading to the active site (Figure **2.2**). Electrostatic interactions between these residues and protonated amines are thought to be the mechanism by which AO substrates locate this channel and access the active site. The amine-substrates are deprotonated at the channel entrance and are guided to the cofactor site through hydrophobic interactions with residues in the interior of the cavity. Since this channel is the pathway to the active site,

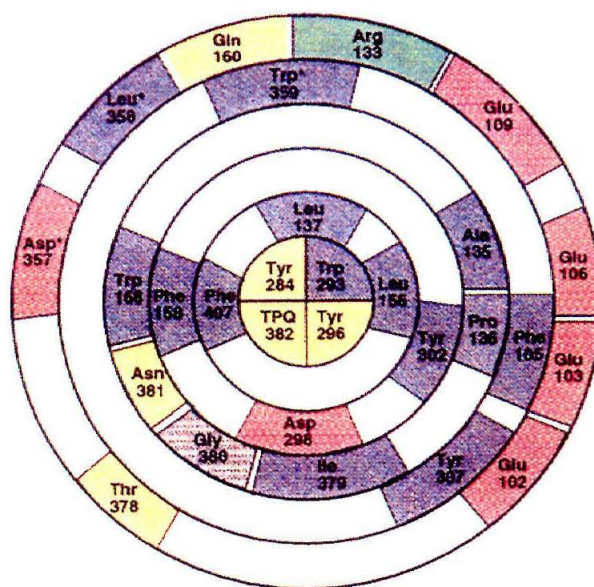


**Figure 2.2:** Residues comprising the channel of AGAO from the surface to the active site. Residues are color coded. Blue: hydrophobic, Red: acidic, Green: basic, Yellow: polar uncharged, Gray: glycines



it was expected to provide the best route for electron transfer to the site as well. Proper orientation of this region at the electrode surface is thus crucial to obtaining electrochemical signals from AO cofactors. The electrostatic charge at the channel entrance was considered in the choice of electrodes and modifiers. In studies with edge-plane graphite electrodes,  $\text{Mg}^{2+}$  ions were added to the protein solution. This creates a cationic layer at the electrode surface, which attracts the negative patch that is associated with the AO channel. For studies using gold electrodes, several amine-terminated modifiers were chosen that could interact with AO in a similar fashion as the substrates. A pyridyl complex (pyridine 4-aldehyde thiosemicarbazone: PATS-4) and two peptide modifiers (KCTCCA and  $(\text{KC})_2$ ) were used. These complexes bind to the gold surface via sulfur atoms.

### *Materials and methods*

*Protein samples:* Samples of purified protein were obtained from D. M. Dooley and his group at Montana State University; the general methods for protein purification are described in Appendix A. The concentrations of either AGAO or BPAO used in the electrochemical experiments, ranged from 300 to 500  $\mu\text{M}$  in 0.1 M potassium phosphate buffer ( $\text{KPi}$ ), pH 7. Protein concentrations were determined as described in Appendix A.

*Modifiers:* Pyridine 4-aldehydethiosemicarbazone (PATS-4) and the KCTCCA peptide modifier were purchased from Sigma-Aldrich. The  $(\text{LysCys})_2$  peptide was synthesized at the Peptide Synthesis Facility at Caltech. Purity was determined by HPLC and mass spectral analysis.



A ( $\text{KP}_i$ , pH 7) 0.1 M ionic strength solution was employed in all experiments. When  $\text{Mg}^{2+}$  was required, a solution of  $\text{MgCl}_2$  (1M: 15–30  $\mu\text{L}$ ) was added to the samples.

### *Electrochemistry*

*Apparatus and measurements:* Cyclic voltammetry (CV) and Osteryoung square-wave voltammetry (OSWV) were performed on a Bioanalytical Systems (BAS) CV50-W electrochemical analyzer. The electrochemical cell consisted of a small volume (200–300  $\mu\text{L}$ ), three-electrode, two-compartment glass cell. A Standard Calomel Electrode (SCE) served as the reference electrode and Pt wire was the auxiliary electrode. The reference compartment was separated from the working solution by a modified Luggin capillary. All solutions were deoxygenated by flowing Ar over the samples for at least 30 min. In cases where  $\text{Mg}^{2+}$  ions were used, a small volume ( $\sim$  15–30  $\mu\text{L}$ ) of a 1M  $\text{MgCl}_2$  solution in water was added to the samples.

### *Electrode preparations*

*Edge-plane graphite electrodes:* Edge-plane graphite electrodes (PGE) were prepared by encasing a 5 mm diameter cylinder of PGE into a glass tube, sealed with heat-shrink tubing. Electrical contact to the graphite surface was made with a copper wire in the glass tube, and a small amount of mercury. Electrodes were polished with 0.3  $\mu\text{m}$  alumina, sonicated for at least 20 min and briefly dried with a heat gun immediately before use.

*Modified Au electrodes:* Au electrodes were polished with 0.05  $\mu\text{m}$  alumina and sonicated for  $\sim$  20 min. Electrodes were etched in 1 M sulfuric acid by cycling from -300 mV to 1.5 V (vs. Ag/AgCl). They were subsequently modified with thiol compounds as follows: For PATS-4 modification, electrodes were sonicated in a  $\text{KP}_i$  solution

(containing  $\sim 2$  mg of the compound) for several minutes and stored in the solution until further use. Electrodes modified with the KCTCCA and  $(KC)_2$  peptides were prepared according to procedures described by Hill et al.<sup>4</sup>. Au electrodes were placed in a 2 mM solution of the peptide in  $KP_i$ , and electrochemically modified by cycling the electrode in the solution at reducing potentials (0–800 mV vs. SCE) for  $\sim 10$  cycles. Electrodes were stored in the peptide solutions until further use.

### *Results*

The electrochemistry of AGAO and BPAO was investigated with pyrolytic edge-plane graphite electrodes. Cyclic voltammetry gave no discernible signal. However, redox waves were observed for samples of AGAO by square wave voltammetry. A peak was observed at -0.31 V vs. SCE, which was small in amplitude and poorly defined. Addition of  $Mg^{2+}$  to the solution enhanced this wave dramatically (Figure 2.3). This was an indication that amine oxidase prefers interactions with positively charged groups. An analogous redox couple was not observed for BPAO, however, even upon addition of Mg ions to the solution.

The redox chemistry of the amine oxidases was also investigated on thiol modified gold electrodes. Electrochemistry using both PATS-4 and the KCTCCA peptide as promoters was unsuccessful. For each enzyme a redox couple was observed with  $(KC)_2$  peptide modified electrodes by square wave voltammetry. A broad peak centered around -340 mV (-365 mV) vs. SCE was seen upon reduction of AGAO (BPAO) (Figure 2.4, 2.5), similar to the results with PGE electrodes. Interestingly,

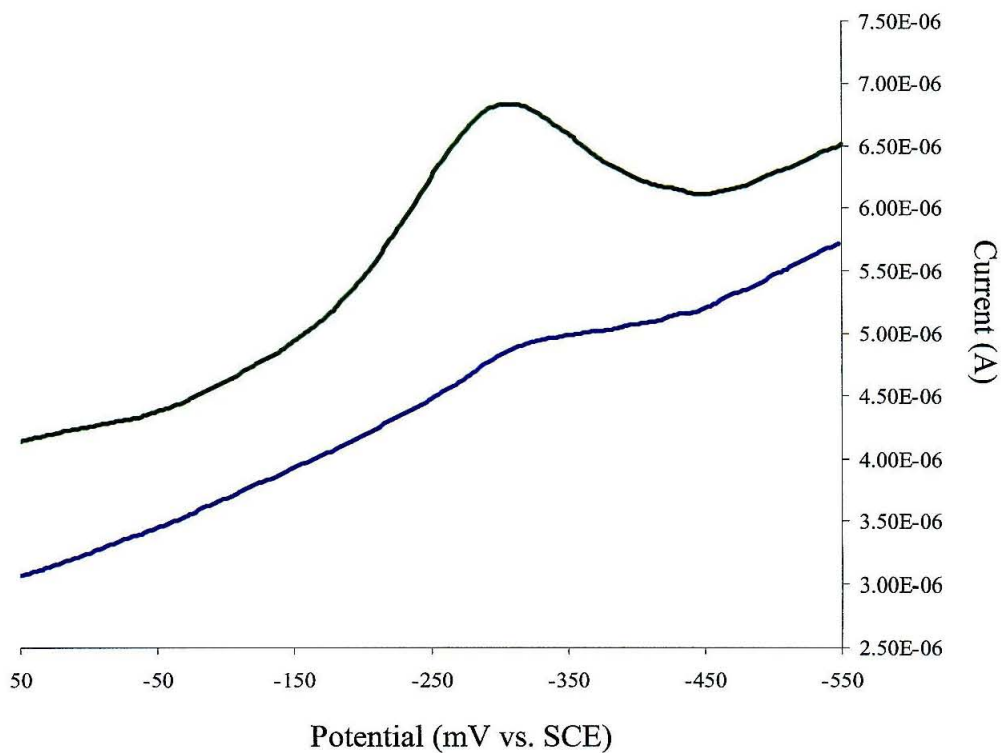


**Figure 2.3:** Square wave voltammograms of AGAO on PGE electrodes:

(-) bare PGE, no  $\text{Mg}^{2+}$ ; (-) 100  $\mu\text{M}$   $\text{Mg}^{2+}$ .

[AGAO] = 500  $\mu\text{M}$ , 0.1 M  $\text{KP}_i$ , pH 7.

$E^{1/2}$  = -310 mV vs. SCE.

Sweep amplitude: 25 mV; sweep frequency: 5 Hz; potential step: 2 mV.

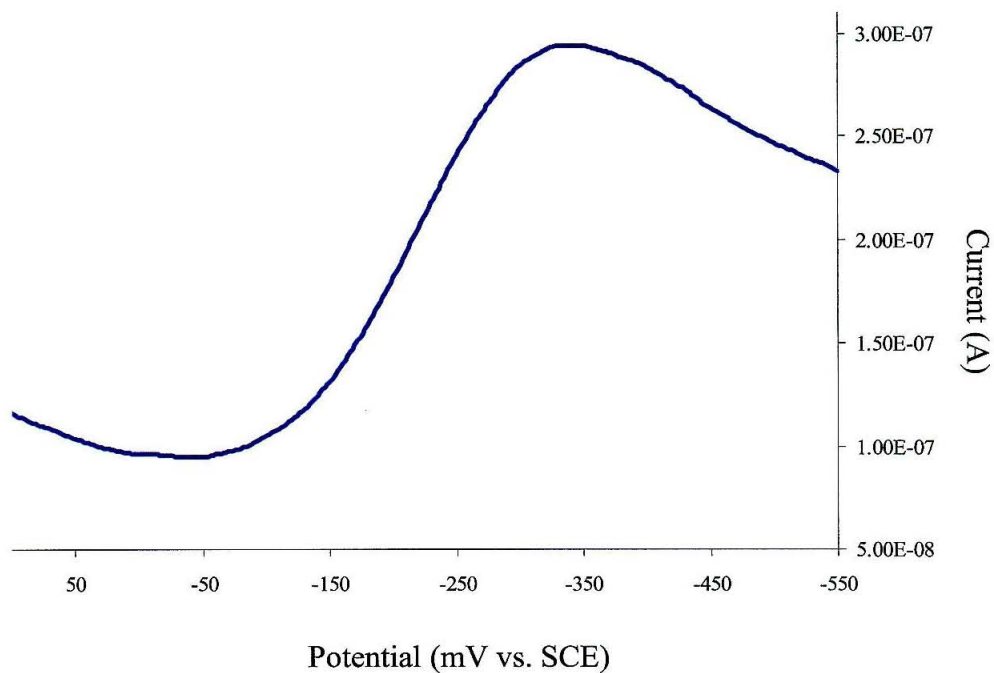


**Figure 2.4:** Square wave voltammogram of AGAO on  $(\text{KC})_2$  modified gold electrode:  $[\text{AGAO}] = 500 \mu\text{M}$ ,  $0.1 \text{ M KPi}$ , pH 7.  $E^{1/2} = -340 \text{ mV vs. SCE}$ . Sweep amplitude:  $25 \text{ mV}$ ; sweep frequency:  $5 \text{ Hz}$ ; potential step:  $2 \text{ mV}$ .

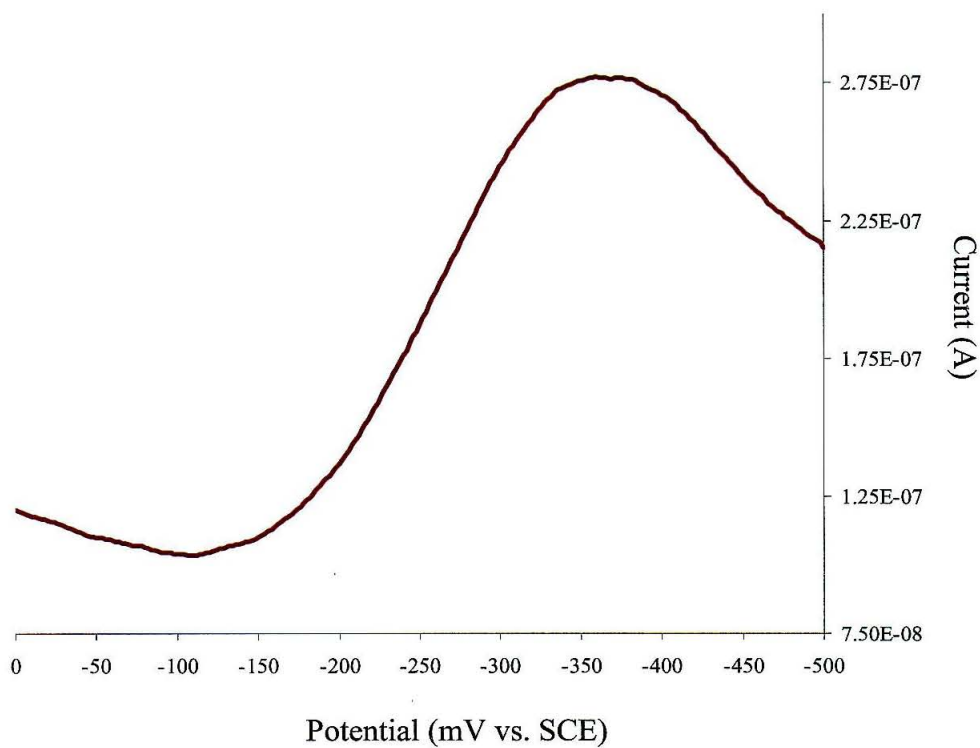


**Figure 2.5:** Square wave voltammogram of BPAO on  $(\text{KC})_2$  modified gold electrode:  $[\text{BPAO}] = 500 \mu\text{M}$ ,  $0.1 \text{ M KPi}$ , pH 7.  $200 \mu\text{M Mg}^{2+}$  added to solution

$E^{1/2} = -365 \text{ mV vs. SCE}$ .

Sweep amplitude:  $15 \text{ mV}$ ; sweep frequency:  $5 \text{ Hz}$ ; potential step:  $2 \text{ mV}$ .



addition of  $\text{Mg}^{2+}$  ions to the BPAO solution improved the signal. In contrast, addition of  $\text{Mg}^{2+}$  to AGAO samples gave poor results.

### *Discussion*

The results of the electrochemical experiments on AGAO and BPAO demonstrate the importance of electrostatic interactions between the protein and the electrode surface. As described previously, the surface environment of the AGAO channel consists of several anionic aspartic and glutamic side chains. These residues are expected to interact favorably with positively charged functionalities, and this is supported by the results at edge-plane graphite electrodes. Studies using bare PGE, having carboxyl groups at the surface, gave poor results. Addition of  $\text{Mg}^{2+}$  ions to the solution led to great improvements in the electrochemistry. The lack of a redox couple for BPAO with PGE electrodes is surprising. This could be due to differences in the surface environment between the two AOs. Although AGAO has a clearly defined acidic patch at the mouth of the channel, this type of patch is not present in all amine oxidases. Electrostatic interactions may play a large role in controlling the substrate specificity of AGAO. However, different interactions could be responsible for the selectivity of other AOs. The surface residues of BPAO may differ considerably from those of AGAO. As a crystal structure of BPAO is not available, the nature of the channel (if one exists) is not known.

In studies using Au electrodes, the  $(\text{KC})_2$  peptide proved to be an effective modifier for both AOs. This is not surprising given that primary amines are the natural substrates for these enzymes. The attraction between the protein and the lysine groups at

the electrode surface is likely to be related to the same interactions that localize amine-substrates to the AO channel. Modification of electrodes with PATS-4 or the KCTCCA peptide was unproductive for measurements of either protein, despite the fact that these complexes also contain amino groups. Possibly these complexes are too hydrophobic in nature, or are not oriented correctly at the electrode surface. Although the nature of their interaction with AO is unclear, it is safe to say that they do not provide a productive surface environment for protein electrochemistry.

The redox couples seen in the electrochemistry of AGAO and BPAO are likely due to the topaquinone cofactor. Comparison with reported potentials for topaquinone model complexes indicates that the values we have obtained are in the right range. A previous investigation of the electrochemistry of PSAO afforded a value of -300 mV vs. SCE for a protein-bound topaquinone<sup>5</sup>, in close agreement with the redox potentials measured for AGAO and BPAO. The voltammograms using PGE and KC modified gold electrodes were unfortunately less than ideal. The redox waves are fairly broad, so information regarding the number of electrons involved or the electrode kinetics could not be extracted.

The poor electrochemical response is presumed to be due to the buried nature of the cofactors. This is a common problem in the direct electrochemistry of enzymes. Unlike electron transfer proteins, the redox site of an enzyme often lies deep within the protein without a well-defined pathway for electron transfer. The crystal structure of AGAO indicates that the cofactor site lies  $\sim 20$  Å beneath the protein surface. The substrate channel provides a route to this site. However, the electrochemistry techniques described above, aid only in making contact with the top of the channel at the electrode

surface. Electrons must still be transferred through the solvent interior, and such reactions through water are fairly slow over this distance<sup>6</sup>. The low rates give poor redox kinetics at the electrode. In light of these factors, we developed a new method that provides direct access to the amine oxidase active site, as described in subsequent chapters.

*References*

- (1) Guo, L.-H.; Hill, H. A. O. In *Adv. Inorg. Chem.*, 1990; Vol. 36, pp 341-375.
- (2) Hill, H. A. O.; Hunt, N. I.; Academic Press, 1993; Vol. 227, pp 501-522.
- (3) Frew, J. E.; Hill, H. A. O. *Eur. J. Biochem.* **1988**, *172*, 261-269.
- (4) Barker, P. D.; Di Gleria, K.; Hill, H. A. O.; Lowe, V. J. *Eur. J. Biochem.* **1990**, *190*, 171-175.
- (5) Sebela, M.; Studnickova, M.; Wimmerova, M. *Bioelectrochemistry and Bioenergetics* **1996**, *41*, 173-179.
- (6) Ponce, A.; Winkler, J. R.; Gray, H. B. *J. Am. Chem. Soc.* **2000**, *122*, 8187-8191.

## **Chapter 3**

### **Design and synthesis of molecular wires for amine oxidases**



Our approach to the amine oxidase challenge was to synthesize a series of “molecular wires” for the purpose of electrochemical and mechanistic investigations. These wires were designed to meet very specific requirements. Their structures must be such that they are able to bind tightly within the AO substrate channel, that is, the molecules must be compatible with the depth and volume constraints of the channel and interact favorably with surface and interior residues. For successful electrochemistry, the wires must provide an electron transfer pathway to the active site with rates superior to those through the solvent or the protein backbone. They must also contain a functionality that binds to gold surfaces. The wires can then be used to generate protein monolayers on electrodes.

Phenyl-ethynyl units were selected to comprise the bridge of the wires. The conjugation supplied by these units imparts strong electronic coupling and promotes rapid rates of electron transfer through the molecule. The electron transfer properties of phenyl-ethynyl oligomers on gold surfaces have been interpreted in terms of an experimental rate/distance decay factor  $\beta$  of  $-0.36 \text{ \AA}^{-1}$ . This  $\beta$  value indicates that electron tunneling rates on the order of  $10^5 \text{ s}^{-1}$  will be observed for an oligomer 20  $\text{\AA}$  in length. It follows that high rates can be expected for electron transfer through this type of bridge from the electrode surface to the active site of an amine oxidase.

The phenyl-based oligomers are expected to fit inside the AGAO substrate channel, since phenethylamine is the natural substrate for this enzyme. Evidence for the ability of the protein to accommodate fairly large molecules is also given by the use of naphthalene-based inhibitors. The AGAO crystal structure also indicates that the path of

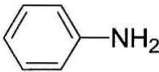
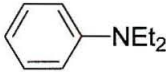
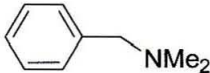
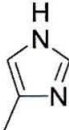
the channel is fairly straight such that flexibility is not required in the molecules. A thiophenol was chosen as the terminal group to bind to the electrode surface. Compared to alternatives such as pyridyl groups, thiols generate the strongest bonds to Au surfaces.

The opposite end of the oligomer serves as the channel-specific group. By definition it must consist of a functional group that can bind specifically to the active site, thereby promoting the insertion of the wire into the protein. It seemed logical to employ an amine group for this purpose, since amines are enzyme substrates. However, we would not like the substrate mimic to engage in reactions with the enzyme, at least not in the first electrochemical experiments. In these experiments, we only want the wire to be a mediator for electron transfer to the redox site, a requirement that suggests the use of tertiary amines. Inhibition studies with a series of N-containing molecules (Table 3.1) provided information on their ability to bind to AGAO; this, in turn, allowed us to determine which group or groups could function as the channel-specific end of the wire. Most of these molecules resemble phenethylamine, and have  $pK_a$  values in the range 4.5 – 10. With this range of  $pK_a$ 's, we can assess the importance of charge in AO interactions with potential inhibitor wires.

#### *Inhibition studies:*

#### *Materials and methods*

Inhibition studies were carried out on AGAO using phenethylamine as the substrate. The rate of  $O_2$  consumption by the enzyme during the reaction with phenethylamine was used as an assay for substrate inhibition of AGAO by the nitrogen-containing compounds in Table 3.1. The rate of  $O_2$  consumption in the presence of the

Molecule	pK <sub>a</sub>	% Inhibition
 Aniline	4.6	35 % at 10 mM
 Diethylaniline	6.7	54% at 100 μM
 Dimethylbenzylamine	9.7	55% at 10 mM
 Imidazole	5.6	50% at 1M *

\* Data not shown

**Table 3.1:** Molecules used for inhibition studies of AGAO.

inhibitor compounds was compared to the rates measured in the presence of phenethylamine alone, and a percent inhibition was calculated from the results.

The concentration of AGAO in the assays was 0.17 mg/mL, and the phenethylamine concentration was 100  $\mu$ M. Inhibitor concentrations ranged from 10  $\mu$ M to 10 mM. Aqueous KPi, 0.1 M ionic strength, pH 7 containing 10% DMSO served as the buffer in all experiments. DMSO was used to solubilize the inhibitor compounds, many of which were otherwise insoluble in aqueous solution. All assays were carried out at 25°C in a sealed cuvette, while stirring.

O<sub>2</sub> consumption assays were performed using a “Microelectrodes” oxygen electrode attached to a voltmeter. The electrode was calibrated by measurement of the voltage at 100%, 21%, and 0% O<sub>2</sub>. For measurements at 100% oxygen, pure O<sub>2</sub> was bubbled through a solution of KPi or KPi with 10% DMSO. Similarly, the 21% O<sub>2</sub> value was measured by bubbling with house air. For the 0% O<sub>2</sub> measurement, dithionite was added to react with O<sub>2</sub> present in solution. The rate of oxygen consumption by the enzyme was determined by measuring the change in potential due to the amount of O<sub>2</sub> over a period of ~ 5–10 min. This was converted to a % O<sub>2</sub> based on the above calibration. The % O<sub>2</sub> was subsequently converted to a concentration of dioxygen ([O<sub>2</sub>]) using the equation:

$$S = (a/22.414) ((760-p)/760) (\%O_2/100),$$

where

$$\begin{aligned} S &= \text{solubility of O}_2 \text{ in moles/ L} = [\text{O}_2] \\ a &= \text{absorption coefficient of O}_2 \text{ at 25 }^\circ\text{C} = 0.02831 \\ p &= \text{the vapor pressure at 25 }^\circ\text{C} = 23.756. \end{aligned}$$



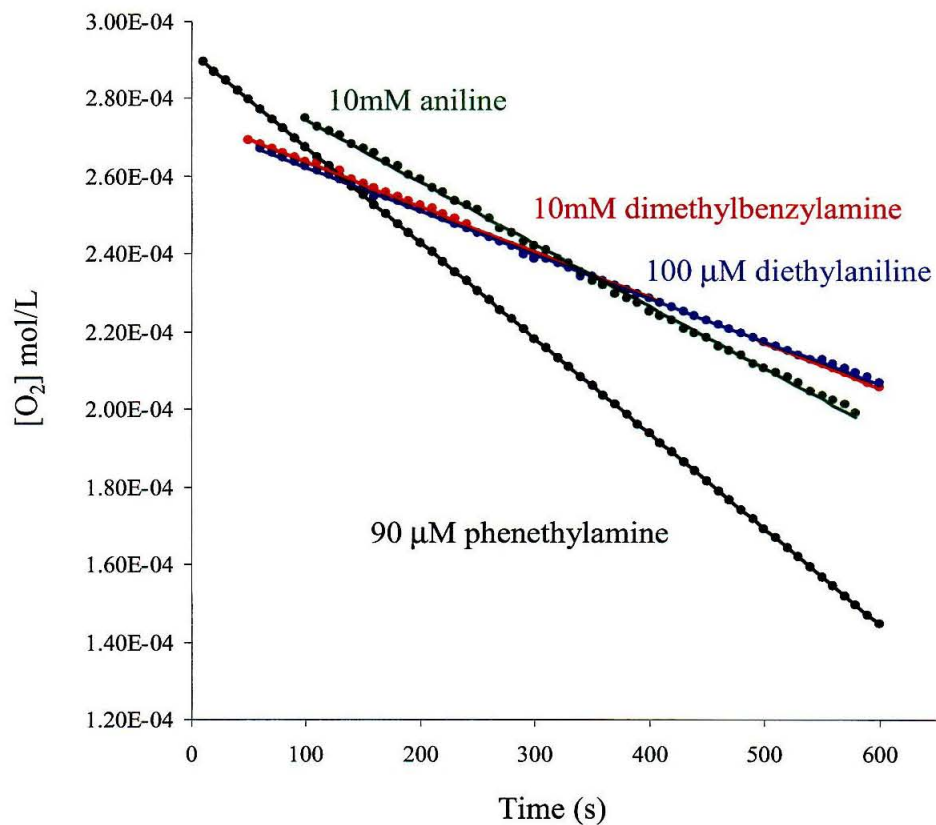
## Results

The results of the inhibition studies are shown in Figure 3.1. Aniline proved to be a poor inhibitor, showing only 35% inhibition at concentrations 100-fold greater than that of the substrate. Dimethylbenzylamine showed slightly better inhibition at this concentration. The addition of 10 mM dimethylbenzylamine resulted in a 55% decrease in enzyme turnover rates. However, the best inhibitor proved to be diethylaniline, which impeded enzyme reactivity by more than 50% at a concentration equivalent to that of the substrate. This suggests that the dissociation constant for diethylaniline is comparable to that of phenethylamine ( $K_d = 9 \mu\text{M}$ ). This result is surprising given that the  $\text{pK}_a$  of diethylaniline is only 6.6, whereas the  $\text{pK}_a$  of dimethylbenzylamine is closer to 10. The charge on the amine has been cited as important for recognition of substrate by the AO channel. In addition, dimethylbenzylamine resembles the AGAO substrate more closely than diethylaniline. However, benzylamine is also a poor substrate for AGAO ( $K_d = 36 \mu\text{M}$ ). So, it is apparent that factors other than charge play a role in AO substrate specificity. Based on the results of these studies, molecules were synthesized containing diethylaniline as the channel-specific terminal group.

## Synthesis of Molecular Wires

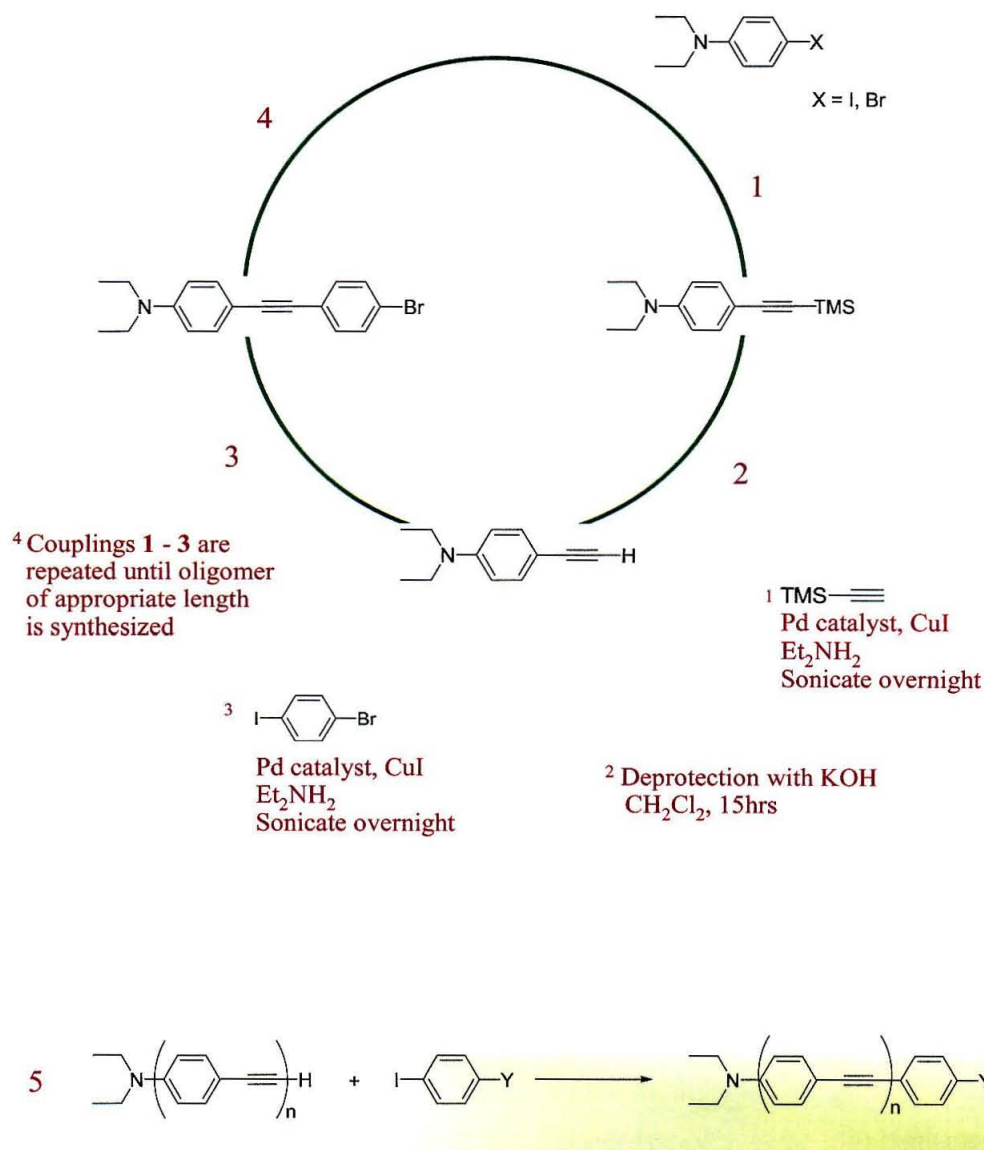
Wires were synthesized by means of Pd-catalyzed cross-coupling reactions (Figure 3.2). Beginning with p-iododiethylaniline, the alkyne unit is added by reaction with TMS-acetylene. Deprotection of the terminal alkyne, followed by coupling with p-iodobromobenzene, affords the bromo-terminated complex. Additional phenyl-alkyne units are added in this manner until an oligomer of the desired length is obtained. The





Molecule	Rate: $\Delta[O_2] \text{ s}^{-1}$
phenethylamine	$2.5 \times 10^{-7}$
aniline	$1.6 \times 10^{-7}$
diethylaniline	$1.16 \times 10^{-7}$
dimethylbenzylamine	$1.12 \times 10^{-7}$



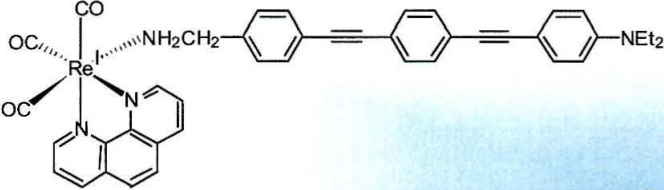
**Figure 3.1:** Results of inhibition studies with AGAO using phenethylamine as the substrate. Buffer: aqueous 0.1 M  $KP_i$ , pH7 containing 10% DMSO.



**Figure 3.2:** Methodology for synthesis of wires by Pd cross-coupling reactions. The reporter group (Y) is attached to the oligomer end, opposite the channel-specific group in the final step (5).

thiol group is appended to the oligomer in the final coupling of the alkyne terminated oligomer with iodothiophenol. A wire consisting of three phenyl units affords a length of  $\sim 24$  Å. This length is ideal given the depth of the AGAO channel, and allows the component opposite the amine functionality to protrude from the cavity. This is crucial for the electrochemical wire, since the thiol group must eventually be attached to an electrode surface.

The methodology for synthesis of the complexes permits incorporation of an array of functionalities in addition to the thiophenol (Figure 3.3). These “reporter” groups can be employed for the study of amine oxidases using a variety of techniques. A benzylamine terminated complex was synthesized for fluorescence binding studies. This compound served as the starting material for synthesis of metal terminated wires for electron transfer experiments. Synthetic and characterization procedures are described in full detail in Appendix B.

Wire	~ Length
 <b>1</b>	22 Å
 <b>2</b>	22 Å
 <b>3</b>	29 Å

**Figure 3.3:** Wires synthesized for communication with the active site of amine oxidases.

*References*

- (1) Creager, S.; Yu, C. J.; Bamdad, C.; O'Connor, S.; MacLean, T.; Lam, E.; Chong, Y.; Olsen, G. T.; Luo, J.; Gozin, M.; Kayyem, J. F. *J. Am. Chem. Soc.* **1999**, *121*, 1059-1064.



## **Chapter 4**

### **Binding of molecular wires to AGAO**

The inhibition experiments detailed in Chapter 3 suggest that molecular wires with tertiary amine termini likely will bind to the substrate channel of AGAO. The next step is to verify that oligomers with this functionality actually reside in the AGAO channel and to acquire information regarding the nature of their association with the enzyme. Accordingly, AGAO-inhibition and wire-fluorescence experiments studies were performed with solutions containing both enzyme and wire.

The absorption spectrum of AGAO exhibits a band at 480 nm due to the topaquinone cofactor. This enables fluorescence energy transfer studies with AO, in which the TPQ acts as a quencher for fluorescent probes that emit in this region. The benzylamine terminated complex, DEA-1-BzA (Compound 2, Figure 3.3), was synthesized for the purposes of these studies. Initially, this complex was designed for functionalization with the fluorophore 5-((((2-iodoacetyl)amino)ethyl)amino)naphthalene-1-sulfonic acid (1,5-IAEDANS). Fluorescence due to the dansyl group occurs at 490 nm and thus has significant overlap with TPQ absorption. However, attachment of the fluorophore to the benzylamine oligomer seemed to prohibit protein binding (data not shown). This was presumed to be due to the flexibility of the dansylated molecule, which allowed “self-stacking” of the naphthyl group and the phenyl rings of the oligomer. The complexes are not very soluble in aqueous solution. Aggregation phenomenon has been observed during studies of the phenyl-ethynyl oligomers and is not unlikely for the dansylated compound. Self-stacking would result in a conformation that would render the complex too bulky for insertion into the protein. The phenyl-ethynyl complexes are highly fluorescent even without the addition of other fluorophores. The benzylamine

terminated wire has an emission maximum at  $\sim 410$  nm in aqueous solution (Figure 4.1). Topaquinone can serve as a quencher of the fluorescence due to DEA-1-BzA as well. Since the fluorescence energy transfer rate is dependent on the distance between the donor and acceptor ( $k \propto (1/r)^6$ ), we expected to obtain information regarding the proximity of the wire to the TPQ. Fluorescence quenching could thus serve as an indicator of the extent of binding within the AGAO channel.

### *Materials and Methods*

Time-resolved fluorescence measurements were performed using the third harmonic of a mode-locked Nd:YAG laser ( $\lambda_{\text{ex}} = 355$  nm) for excitation, and a picosecond streak camera (Hamamatsu C5680) for detection. Fluorescence was selected with a long-pass 400 nm cutoff filter. Steady state fluorescence spectra were recorded on a Hitachi F-4500 spectrofluorimeter ( $\lambda_{\text{ex}} = 320$  nm); absorption spectra on a Hewlett-Packard 8452 diode array spectrophotometer. Steady state spectra were corrected for the fluorescence due to AGAO upon excitation at 320 nm.

Substrate inhibition experiments were performed by measuring the O<sub>2</sub> consumption rate by the enzyme as described in Chapter 3, using 100  $\mu\text{M}$  phenethylamine as the substrate. Concentrations of DEA-1-BzA were 50  $\mu\text{M}$  and 100  $\mu\text{M}$ .

Stock solutions of DEA-1-BzA were prepared in DMSO. Samples containing DEA-1-BzA were prepared in aqueous 0.1 M  $\text{KPi}$ , pH 7 containing 1% DMSO. Time-resolved fluorescence measurements were made in  $\text{D}_2\text{O}$  buffer solutions, to cut down on Raman scattering from  $\text{H}_2\text{O}$ .

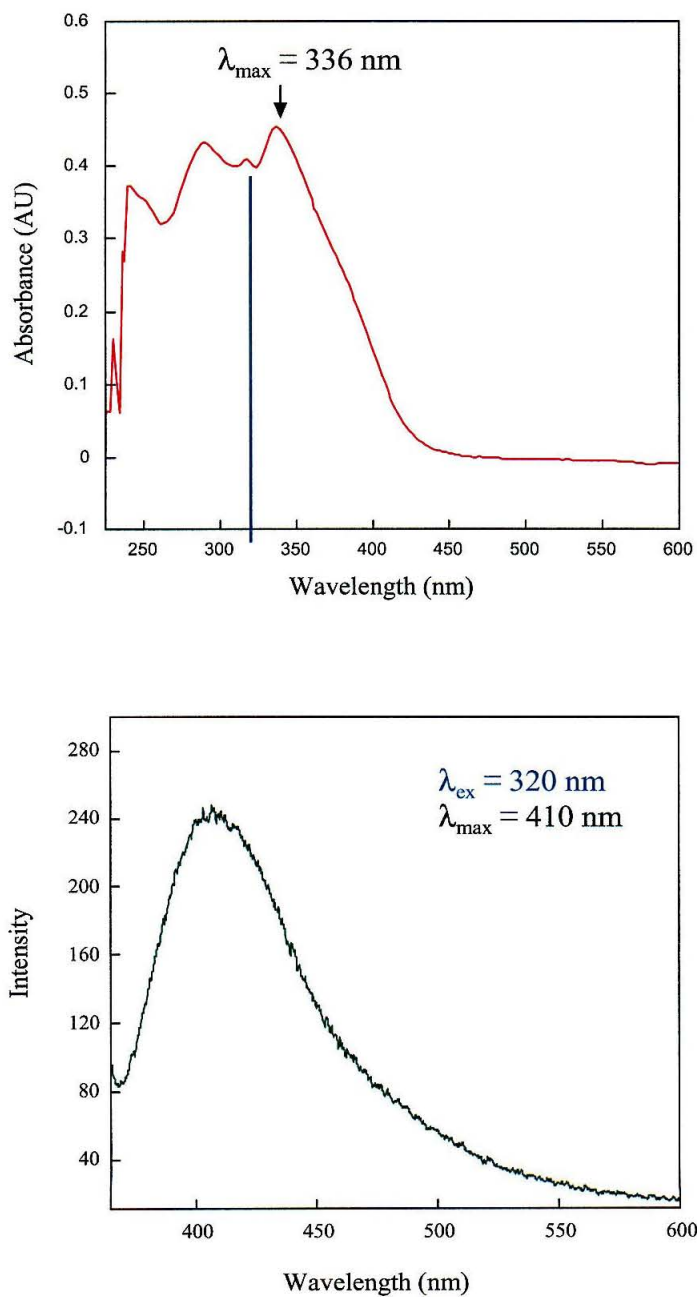


**Figure 4.1:** Absorption spectrum (top) and emission spectrum (bottom) spectra of DEA-1-BzA in aqueous 0.1 M  $\text{KP}_i$ , 10% DMSO solution.

## *Results and Discussion*

The effect of protein binding on the emission decay rate of DEA-1-BzA was investigated by time-resolved fluorescence spectroscopy. The results are shown in Figure 4.2. The free wire decays in less than 5 ns. Contrary to expectations, the apparent lifetime of emission is not altered in the presence of protein. However, a decrease in the fluorescence intensity is observed. This was the first indication that the complex might be bound to the protein. The intensity change suggests that the fluorescence seen in the presence of AGAO is due to free DEA-1-BzA in solution, whereas fluorescence of the bound wire is completely quenched. This requires that the emissive decay rate due to bound DEA-1-BzA be on the order of  $5 \times 10^{10}$ .

Fluorescence quenching by AGAO was further investigated by steady state fluorescence experiments (Figure 4.3). The observed intensity of DEA-1-BzA fluorescence correlates with the amount of AGAO present. Addition of one equivalent (two active site equivalents) of AGAO to a 20  $\mu$ M solution of DEA-1-BzA results in a 75% decrease in fluorescence intensity compared to the wire only solution. Addition of the second protein equivalent completely quenches the fluorescence. These results provide further evidence for binding of the oligomer to the enzyme.

The fluorescence results do not provide unequivocal proof of binding of DEA-1-BzA within the protein channel. However, given the degree of fluorescence quenching in the presence of AGAO, the complex is presumed to be in close proximity to the TPQ cofactor. Association of the wire with the protein surface should not lead to a perturbation of the emission to this extent. As the rates for the “bound wire” were too high to allow an estimate for the lifetime, kinetics data for DEA-1-BzA binding could



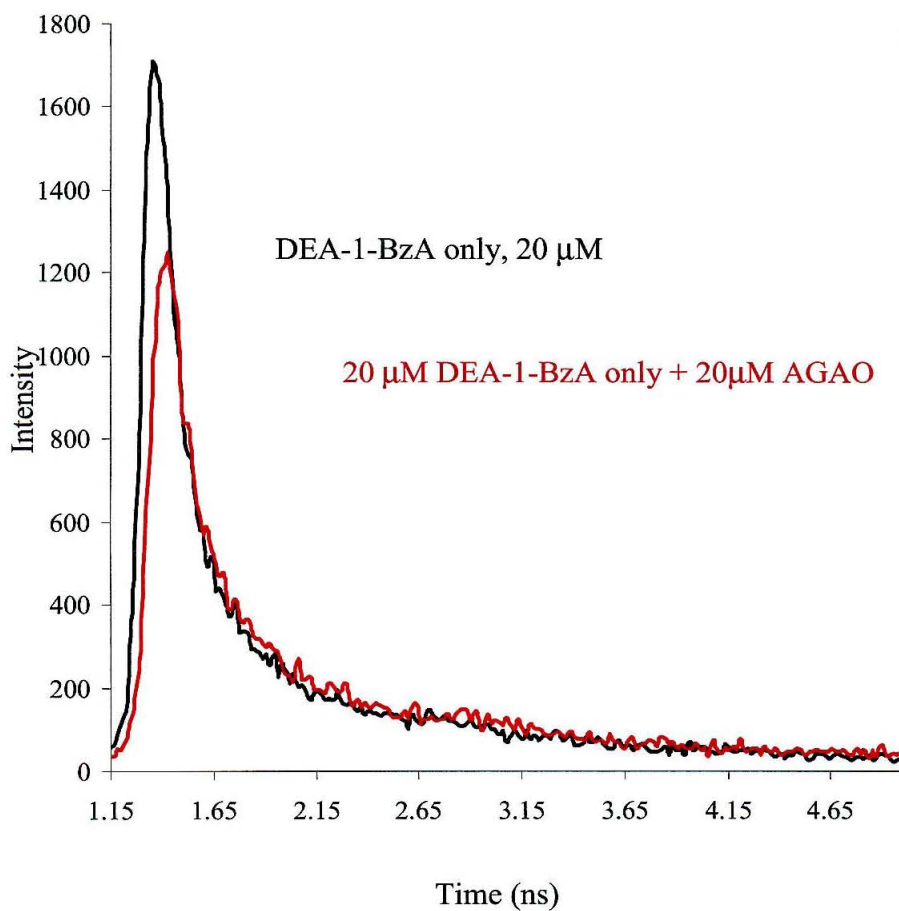


**Figure 4.2:** Time-resolved fluorescence quenching of DEA-1-BzA by AGAO, in deuterated aqueous 0.1 M,  $\text{KP}_i$ , pH 7 solution.  $\lambda_{\text{ex}} = 355 \text{ nm}$ ; 400 nm cutoff filter.

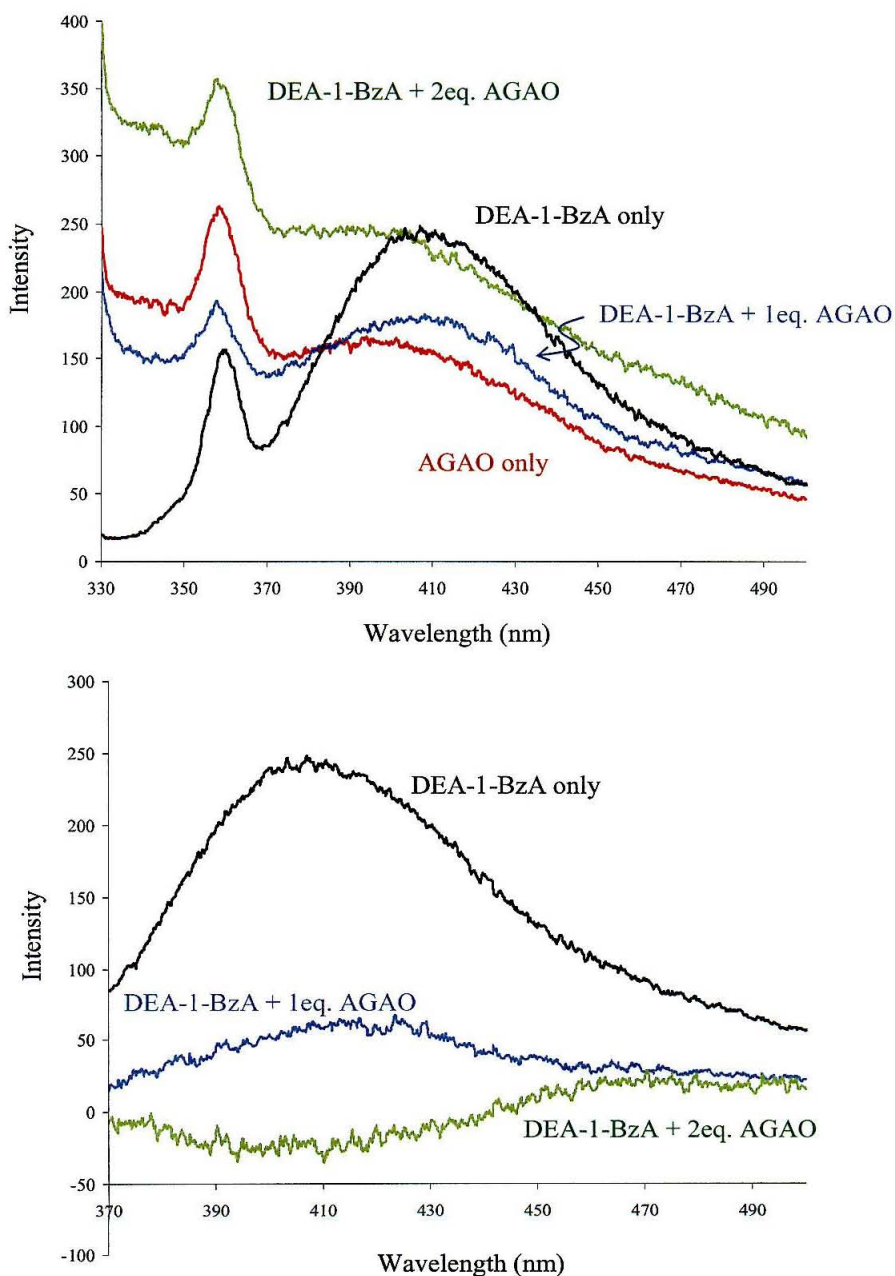
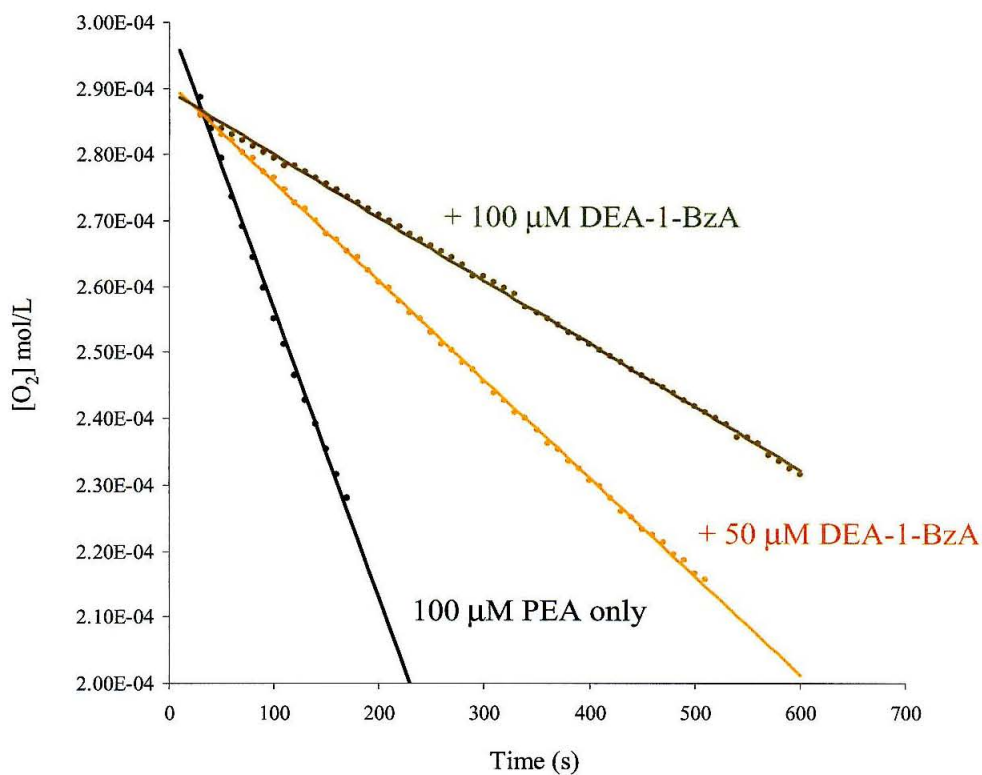


**Figure 4.3:** Steady-state fluorescence quenching of DEA-1-BzA by AGAO. Top: Uncorrected spectra; Bottom: Spectra corrected for fluorescence due to the protein.  $\lambda_{\text{ex}} = 320 \text{ nm}$ .  $[\text{DEA-1-BzA}] = 20 \mu\text{M}$  in aqueous  $0.1 \text{ M KP}_i$ , pH 7 containing 1% DMSO.

not be obtained. Substrate inhibition studies of the benzylamine wire were carried out to probe the protein/wire interaction in greater detail. Inhibition of substrate turnover by the complex implies insertion of the complex into the channel, blocking the pathway for access of substrate to the active site. The catalytic rates for reaction of AGAO with phenethylamine were measured in the presence of DEA-1-BzA. A 65% and 75% reduction in rates was observed in the presence of 50  $\mu\text{M}$  and 100  $\mu\text{M}$  wire, respectively, compared to the rate for 100  $\mu\text{M}$  phenethylamine alone (Figure 4.4). These results suggest that DEA-1-BzA binding is tighter than that of phenethylamine, and place the dissociation constant in the 10  $\mu\text{M}$  range.



[DEA-1-BzA]	Rate: $\Delta[O_2] \text{ s}^{-1}$	% inhibition
0	$4.4\text{e-}7$	-
50 mM	$1.5\text{e-}7$	65 %
100 mM	$9.6\text{e-}8$	78 %

**Figure 4.4:** Results of inhibition studies of AGAO with DEA-1-BzA. 100  $\mu$ M phenethylamine (PEA) was used as the substrate. Studies carried out at 25°C, in aqueous 0.1 M  $KP_i$  containing 1% DMSO.

## **Chapter 5**

### **Photochemical investigations of Re(BzA-1-DEA) with AGAO**



We have synthesized a Re-terminated oligomer (Re(BzA-1-DEA), compound **3**, Figure 3.3), with the ultimate goal of performing electron transfer studies on amine oxidases. Since rapid oxidation or reduction of the active site could be triggered by the Re complex, the oligomer seemed suitable for study of the topaquinone biogenesis mechanism. The first, rate-limiting step in formation of the cofactor is activation of a Tyr residue by the Cu site. Slow rates for this step have, thus far, precluded detection of ensuing intermediates and the role of Cu in the reaction is also ill-defined. Cu may be required only for the initial activation of Tyr, rendering it more reactive towards O<sub>2</sub>. In this case, the Tyr residue could potentially be activated by an external oxidant and formation of TPQ would proceed even in the absence of Cu. Electron transfer studies with Re(BzA-1-DEA), in which Re serves as the one-electron oxidant in a Ni substituted precursor AO, could test this premise. The oxidation of tyrosine occurs at a potential of  $\sim 1$  V vs. NHE. The Re<sup>III/I</sup> potential is estimated as  $\sim 2$  V vs. NHE; thus a photooxidized Re complex could easily oxidize this residue. A related Re complex, Re<sup>I</sup>(phen)(CO)<sub>3</sub>(OH<sub>2</sub>), has been used to label a blue copper protein, *P. aeruginosa* azurin. Oxidative flash quench experiments on Re-azurin have led to the generation of tyrosyl radicals<sup>1</sup>. Rapid electron tunneling rates through the Re-substituted oligomer would permit detection of intermediates formed subsequent to the initial oxidation of tyrosine in precursor AO.

### *Modeling of Re(BzA-1-DEA) into the AGAO Channel*

The Re-terminated wire was modeled into the AO substrate channel using the crystal structure of AGAO (Figure 5.1). The model indicates an excellent fit of the complex within the channel interior. A tyrosine residue (Tyr296) located at the bottom of the channel, adjacent to the active site, acts as a gate that prevents direct contact of the wires with the cofactors. The flexibility of the residue is suggested to play a role in controlling movement of substrates and product in and out of the enzyme<sup>2</sup>. Crystal structure studies of the amine oxidase from ECAO, have demonstrated that the Tyr gate in this enzyme can rotate to allow molecules to access the topaquinone<sup>3</sup>. It is likely that the gate moves upon binding the wires, allowing them to approach the active site more closely. In the absence of a crystal structure of a wire:AO conjugate, this cannot be confirmed.

The (phen)(CO)<sub>3</sub>Re<sup>I</sup>(BzAXDEA) wire was synthesized by reaction of DEA-1-BzA with (phen)Re<sup>I</sup>(CO)<sub>3</sub>(OH<sub>2</sub>) (see Appendix B). In initial experiments, we examined the binding of the wire to AGAO. Careful characterization of the photophysics of this complex is also necessary to be able to interpret the results of photochemistry with the AO active site. Thus the photophysics of Re(BzA-1-DEA) and the effects due to the interaction of the wire with AGAO were investigated, and the results are detailed in this chapter.

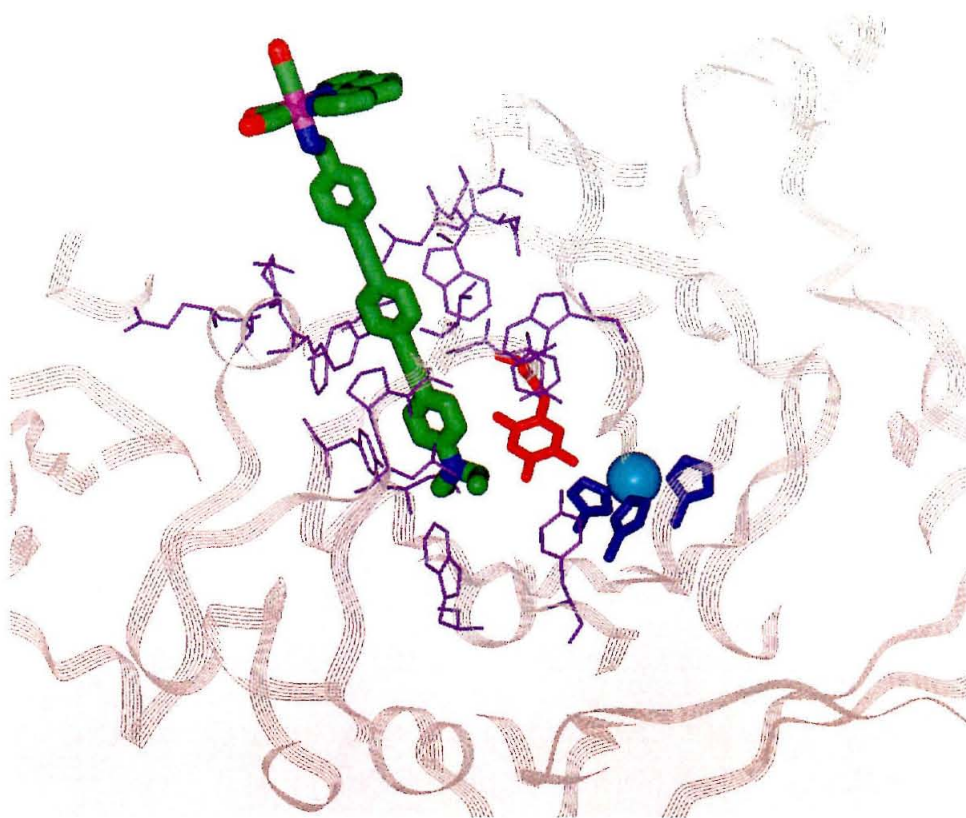


**Figure 5.1:** Re-terminated wire, Re(BzA1DEA), modeled into the AGAO substrate channel. Channel residues are shown in purple, the topaquinone cofactor is colored red, and the Cu site is in blue.

## *Materials and methods*

Re(BzAXDEA) was synthesized from the benzylamine terminated oligomer (**1**) as described in Appendix B.

Absorption spectra were recorded on a Hewlett-Packard 8452 diode array spectrophotometer and emission spectra on a Hitachi F-4500 spectrofluorimeter. Transient absorption spectra were measured on an instrument previously described<sup>4</sup>. The excitation source was the third harmonic of a Q-switched Nd:YAG laser ( $\lambda = 355$  nm).

Aqueous samples of Re(BzAXDEA) were made in 0.1 M  $\text{KPi}$ , pH 7, containing 10% dioxane (or dimethylformamide) to solubilize the complex. Spectrograde dioxane (Burdick and Jackson) and dmf (Sigma-Aldrich) were used for preparation of samples for spectroscopic measurements. The AGAO concentration in the transient absorption experiments was 2.5  $\mu\text{M}$ . All samples were deoxygenated by purging with Ar.

## *Results*

The absorption spectra of the  $\text{Re}^{\text{I}}$  complex, along with those of the precursor compounds ( $((\text{phen})\text{Re}^{\text{I}}(\text{OH}_2)(\text{CO})_3$  and DEA-1-BzA (**2**)), are shown in Figure 5.2. The spectrum of the product resembles the combined spectra of the starting compounds. The free wire has an extinction coefficient of  $2 \times 10^5 \text{ M}^{-1} \text{ cm}^{-1}$  at  $\lambda = 350$  nm, whereas  $\epsilon = 5 \times 10^4 \text{ M}^{-1} \text{ cm}^{-1}$  for the Re functionalized wire. Re(BzA-1-DEA) is highly fluorescent in organic solvents;  $\lambda_{\text{max}} = 440$  nm upon excitation at 355 nm (Figure 5.3A), analogous to DEA-1-BzA. This fluorescence is absent in aqueous solution, and only very weak emission is observed at 600 nm (Figure 5.3B). By comparison with the emission spectra



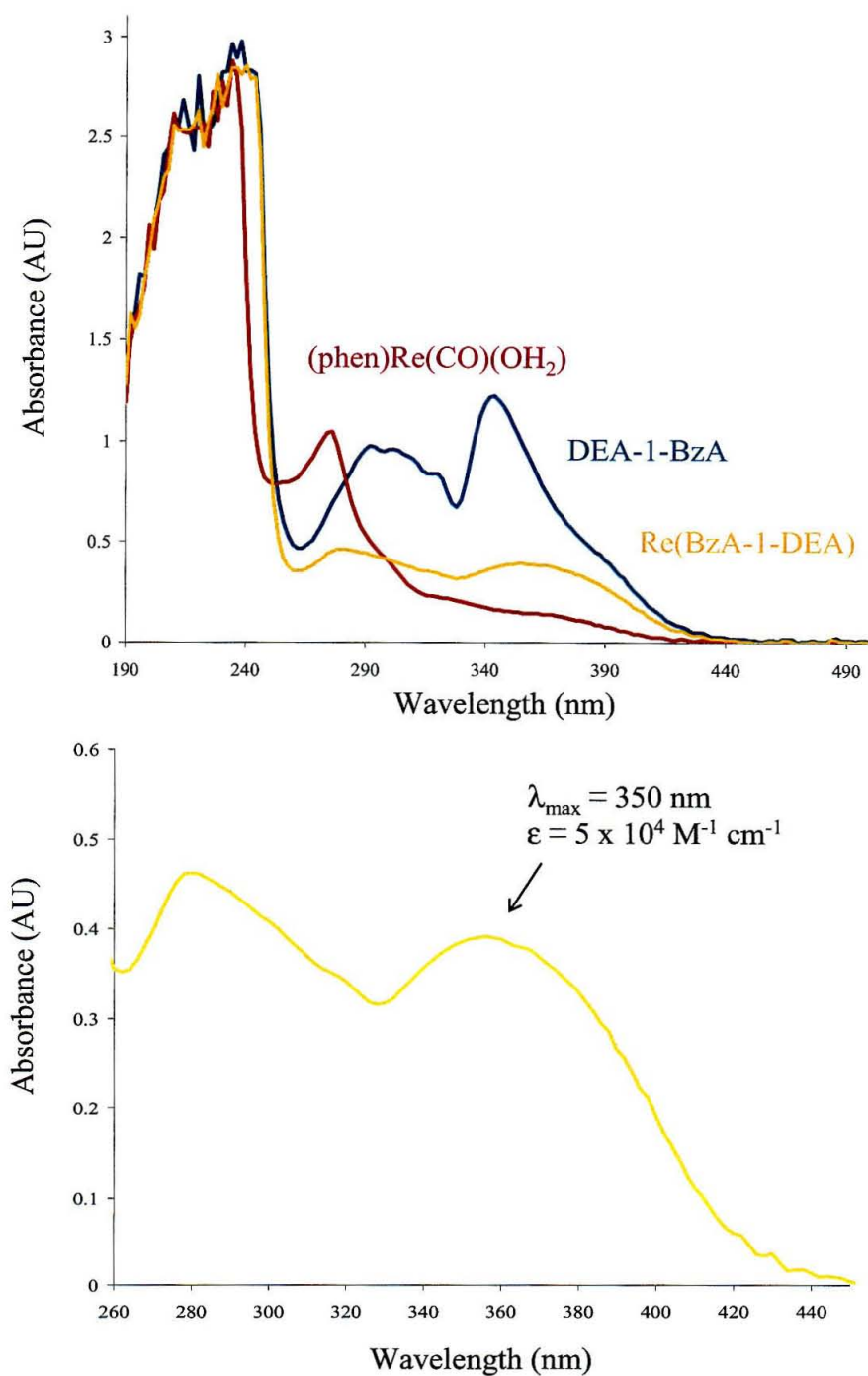


**Figure 5.2:** Top: Comparison of absorption spectrum of Re(BzA-1-DEA) to Re(OH<sub>2</sub>) and DEA-1-BzA. Bottom: Spectrum of 20  $\mu$ M Re(BzAXDEA) in 10% dmf / 90% aqueous 0.1 M KP<sub>i</sub>, pH 7.



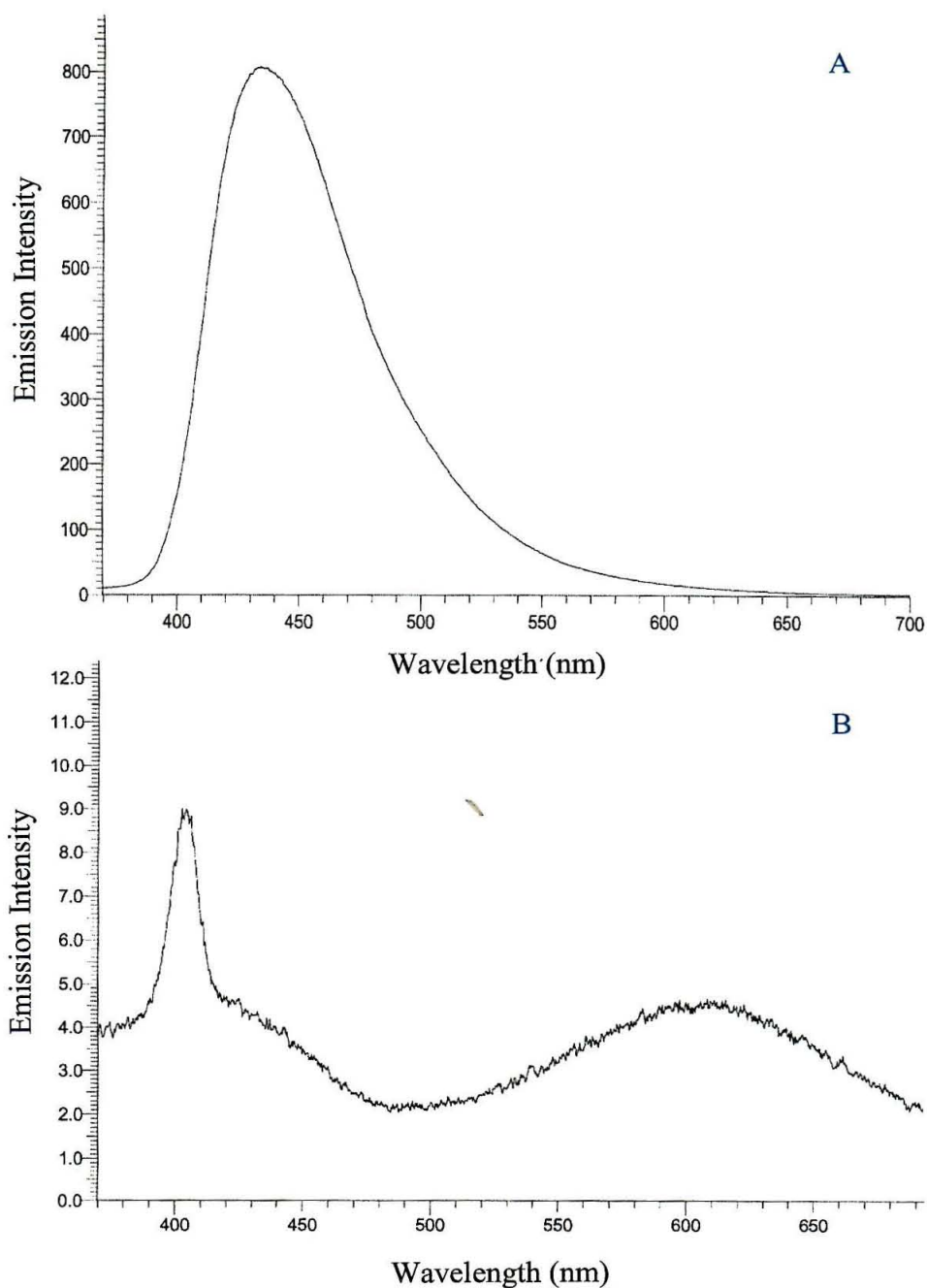


**Figure 5.3:** A) Emission spectrum of Re(BzA-1-DEA) in dioxane:  
B) Emission spectrum in 10% dioxane / 90% aqueous 0.1 M  $\text{KP}_i$ , pH 7  
 $\lambda_{\text{ex}} = 355$  nm.

of DEA-1-BzA and (phen)Re<sup>I</sup>(OH<sub>2</sub>)(CO)<sub>3</sub>, the fluorescence at  $\lambda = 440$  nm seems to be derived from the phenyl-ethynyl unit, whereas the fluorescence at 600 nm is Re based.

The photophysical properties of the Re(BzA-1-DEA) wire were studied by transient absorption spectroscopy. Upon excitation at 355 nm, the compound exhibits a long-lived transient that decays with a rate constant on the order of  $10^5$  s<sup>-1</sup> (Figure 5.4) in organic solvents. This transient is observed in aqueous solution as well, but it decays at a much faster rate (Figure 5.5).

The interaction between the Re-wire and AGAO was investigated by transient absorption spectroscopy. Addition of AGAO to a solution of Re(BzA-1-DEA) leads to slower decay rates for the transient signal (Figure 5.5, 5.6). This can be fit to a biexponential decay function, which yields rate constants of  $2 \times 10^7$  and  $2 \times 10^6$  s<sup>-1</sup> for this process. The fluorescence of the Re-wire is restored by addition of protein (Figure 5.7). The emission decay rate was too fast to measure accurately and is presumed to be greater than  $10^9$  s<sup>-1</sup>.

## Discussion

### *Photophysics of Re(BzA-1-DEA)*

The absorption spectra of the Re-wire exhibits two bands ( $\lambda_{\text{max}} = 280$  nm and 350 nm). The lower energy band is commonly observed in the spectra of phenyl-ethynyl oligomers<sup>5</sup>, and arises from intraligand  $\pi \rightarrow \pi^*$  transitions. Excitation into this transition in THF results in intense emission with a maximum at 440 nm. Intense emission also is a general feature of Re-oligomers, in which the phenyl-ethynyl units are constructed off the 5,5'- positions of the bipyridine of (bpy)Re(CO)<sub>3</sub>Cl. These Re-oligomers have been

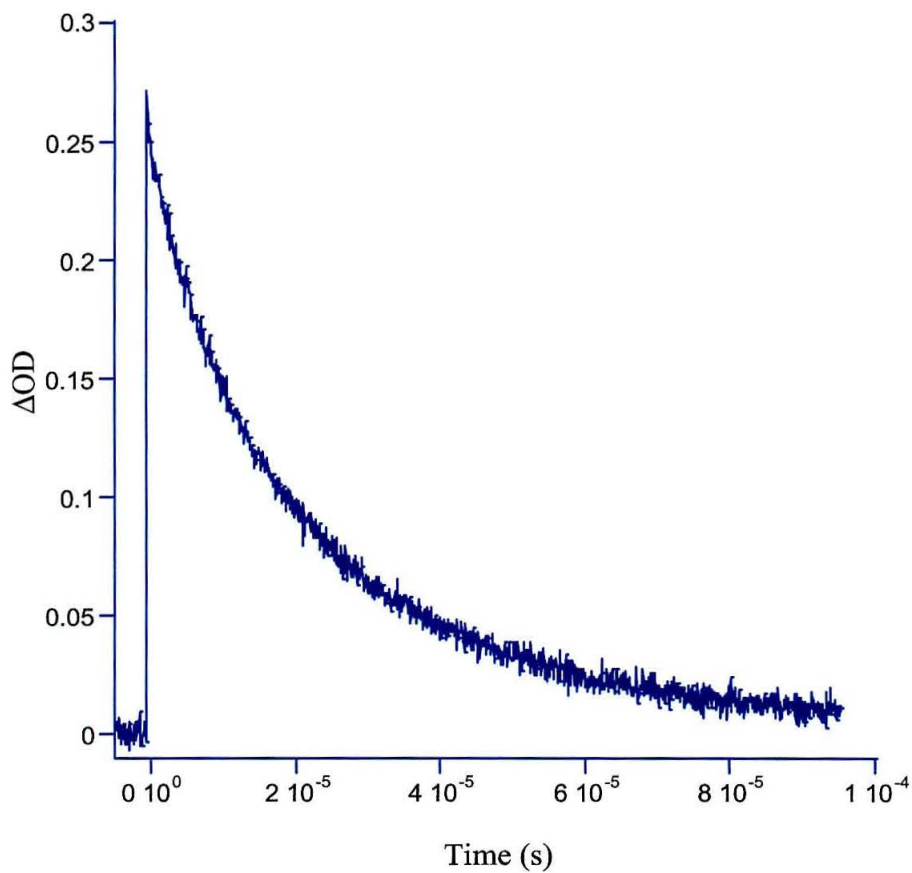


**Figure 5.4:** Transient absorption spectrum of Re(BzA-1-DEA) in dioxane.  $\lambda_{\text{ex}} = 355 \text{ nm}$ ;  $\lambda_{\text{obs}} = 550 \text{ nm}$ ;  $k_{\text{obs}} = 4.8 \times 10^5 \text{ s}^{-1}$ .

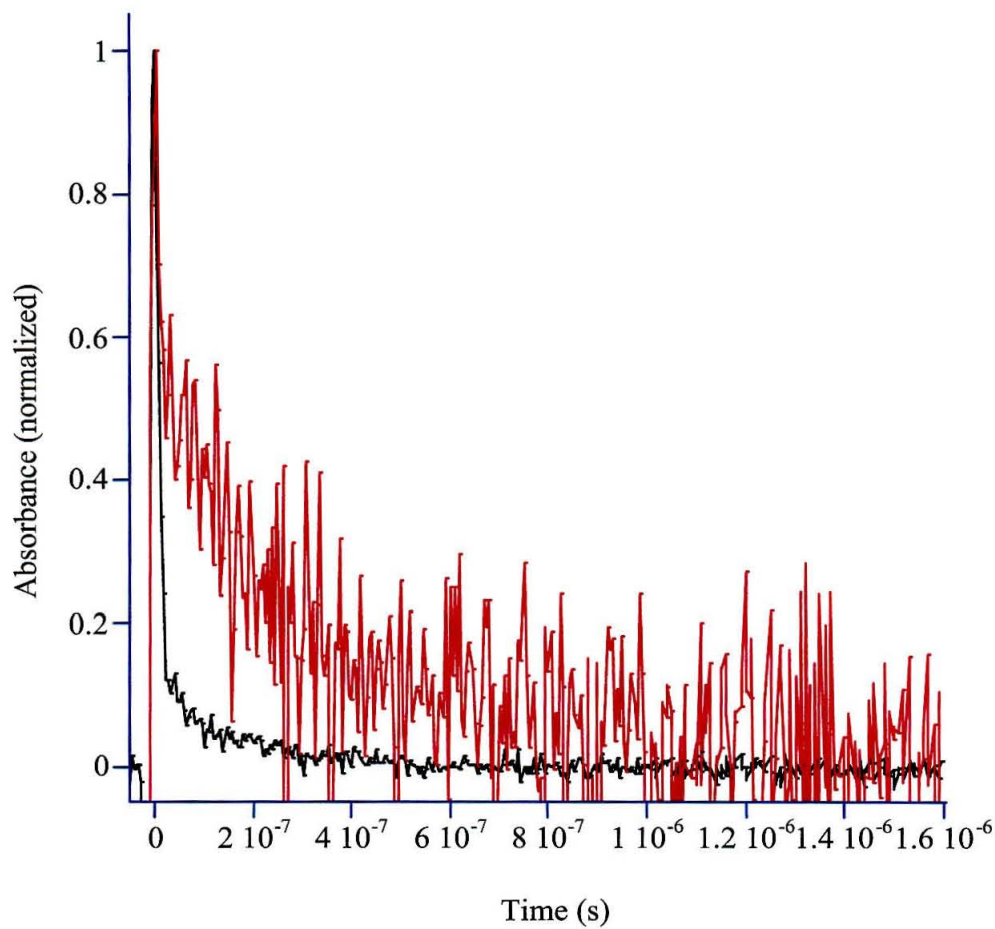


**Figure 5.5:** Transient absorption spectra: (-) 10  $\mu\text{M}$  Re(BzA-1-DEA)  
 ; (-) 10  $\mu\text{M}$  Re(BzA-1-DEA) + 2.5  $\mu\text{M}$  AGAO. Samples in 10%  
 dioxane / 90% aqueous 0.1 M  $\text{KP}_i$ , pH7.  
 $\lambda_{\text{ex}} = 355 \text{ nm}$ ;  $\lambda_{\text{obs}} = 550 \text{ nm}$ .

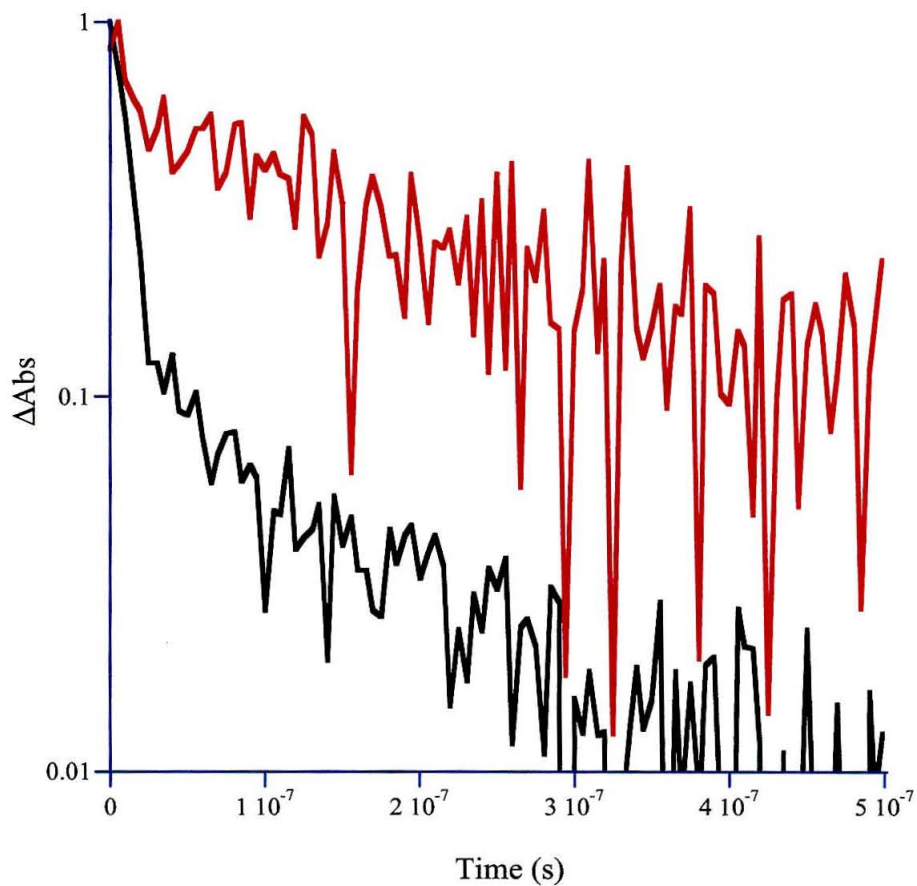


**Figure 5.6:** Log plot of transient absorption spectra: (–) 10  $\mu\text{M}$   $\text{Re}(\text{BzA-1-DEA})$ ; (–) 10  $\mu\text{M}$   $\text{Re}(\text{BzA-1-DEA})$  + 2.5  $\mu\text{M}$  AGAO. Samples in 10% dioxane / 90% aqueous 0.1 M  $\text{KPi}$ , pH 7.  $\lambda_{\text{ex}} = 355 \text{ nm}$ ;  $\lambda_{\text{obs}} = 550 \text{ nm}$ .



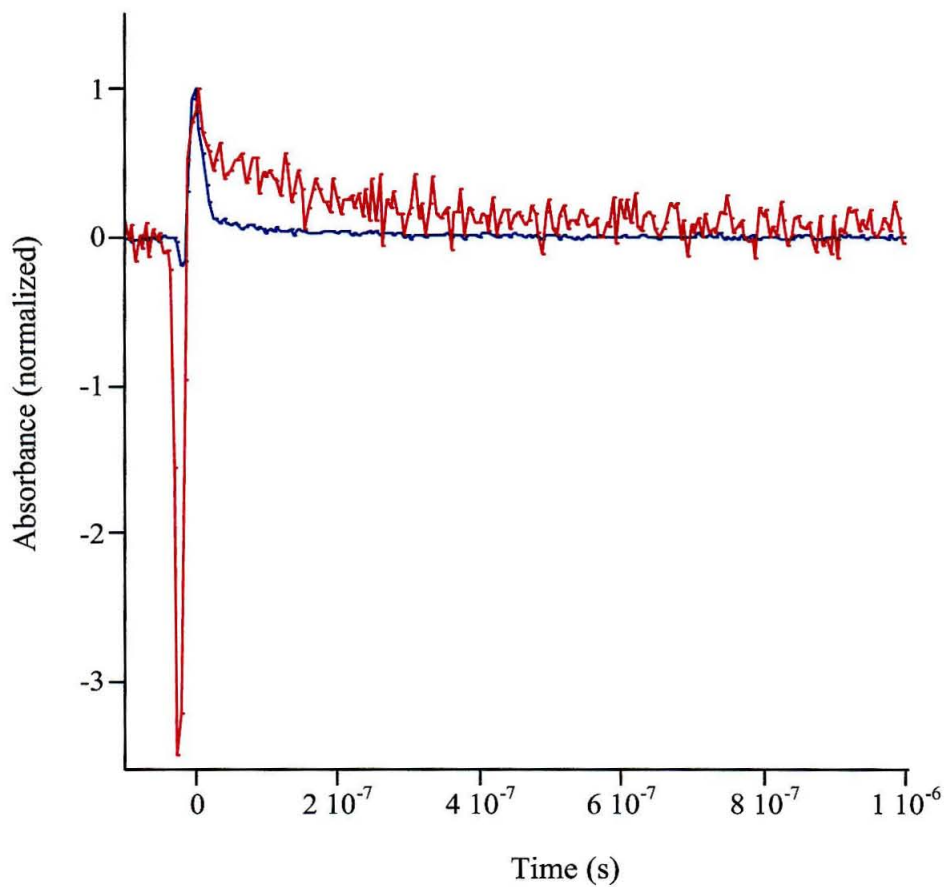


**Figure 5.7:** Transient absorption spectra: (—)  $10 \mu\text{M}$  Re(BzA-1-DEA) ; (—)  $10 \mu\text{M}$  Re(BzA-1-DEA) +  $2.5 \mu\text{M}$  AGAO. Samples in 10% dioxane / 90% aqueous  $0.1 \text{ M}$   $\text{KP}_i$ , pH 7.  $\lambda_{\text{ex}} = 355 \text{ nm}$ ;  $\lambda_{\text{obs}} = 550 \text{ nm}$ .

synthesized by Schanze *et al.*, and their photophysical properties have been investigated<sup>6</sup>. The absorption spectra of the bpy-based Re oligomers are nearly identical with that of Re(BzA-1-DEA). The emission spectra show several interesting differences, however. Upon excitation of the Re-bpy complexes, strong Re-based fluorescence centered around 650 nm is observed, whereas only weak emission is seen at higher energy. In contrast, the fluorescence of Re(BzA-1-DEA) seems to be oligomer-based. Emission at longer wavelengths is not observed for the Re-wire in organic solvents. In aqueous media, weak fluorescence at 600 nm is evident; however, it could be due to trace amounts of free Re-aquo in solution.

The transient absorption behavior of Schanze's complexes provides information regarding the photochemistry that we have observed for Re(BzA-1-DEA). In the former complexes, laser flash photolysis of both the free bipyridine-derived oligomers and the Re complexes affords transients characterized by broad absorption throughout the visible and near-IR region. The lifetime of this transient is  $\sim 400 \mu\text{s}$  for the free bpy-oligomer, and much shorter (20 – 200 ns) for the Re-complexes. The transient was assigned to the  $^3\pi \rightarrow \pi^*$  excited state transition of the oligomer. An analogous transient is also observed upon excitation of Re(BzA-1-DEA), but is much longer lived ( $\sim 100 \mu\text{s}$  in dioxane).

Interestingly the Re(BzA-1-DEA) transient decays rapidly in aqueous solutions. One possible explanation for this behavior could be intramolecular charge transfer to give a complex with positively and negatively charged ends (Figure 5.8). The Re(BzA-1-DEA) complex is unique in that it consists of a high potential Re center as well as an oxidizable amine functionality. In THF, excitation leads to emission from the  $^1\pi, \pi^*$  excited state, which is the fluorescence at 440 nm. Intersystem crossing populates the

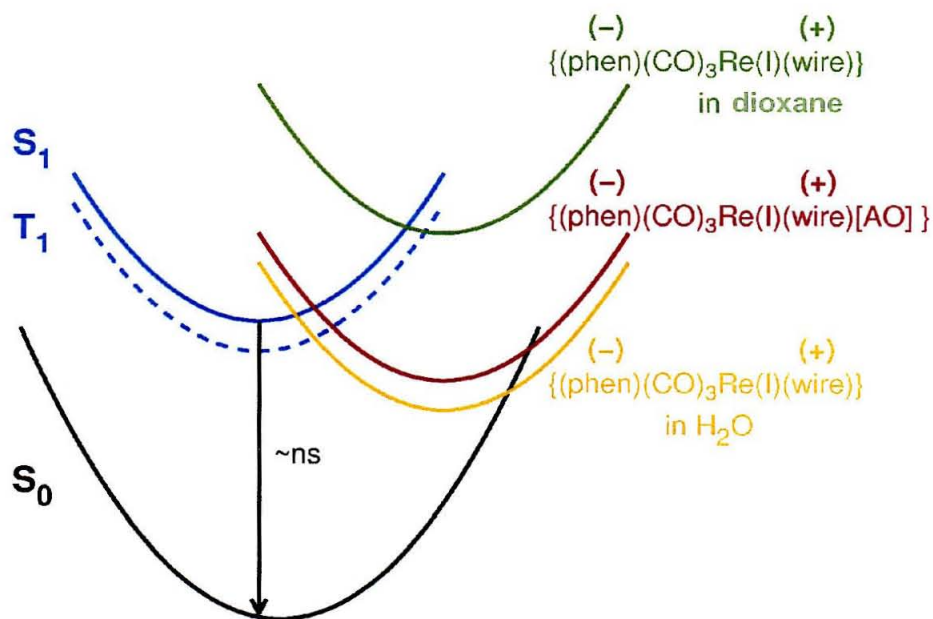


**Figure 5.8:** Diagram for the excited states of  $\text{Re}(\text{BzA-1-DEA})$ , depicting the relative energies. The charge transfer state  $\{(\text{phen})(\text{CO})_3\text{Re}(\text{I})(\text{wire}^+)\}$  is accessible in aqueous media, but is too high in energy in nonpolar solvents.

triplet state ( $^3\pi,\pi^*$ ), which has a transient absorption signature. However, in aqueous media, the charge transfer state should be at much lower energy than in organic solvents, and could be directly accessible from  $^1\pi,\pi^*$ : thus excitation of the Re-wire in aqueous solution leads to population of this state. The species generated by this process can be described as  $[\text{phen}^-](\text{CO})_3\text{Re}[\text{BzA-1-DEA}^+]$ , containing oxidized DEA and reduced phenanthroline. Apparently, this CT state is too energetic to be formed in nonpolar media.

#### *Photophysics of Re(BzA-1-DEA) with AGAO*

Several significant changes are observed in the photophysics of the Re complex in the presence of AGAO. Fluorescence of the Re complex is restored in aqueous solution by the addition of protein to the samples. Addition of AGAO also leads to an increased lifetime for the transient observed upon excitation of the complex. This can be fit to a biexponential decay function, which indicates that there are two separate processes for decay of this species.

The results are suggestive of Re(BzA-1-DEA) binding to the protein. The increased fluorescence and longer lifetime of the transient implies a more hydrophobic environment, consistent with binding of the complex within the AGAO channel. Intense fluorescence and a long-lived transient are only observed when the complex resides in organic solvents. The charge transfer state for enzyme-bound wire lies higher in energy than the CT state of free wire due to the difference in the nature of the surrounding environment. The slower rate of decay from this state could be a manifestation of the Marcus inverted effect<sup>7</sup>.

The results of experiments of the Re-wire with AGAO are promising: the binding of Re(BzA-1-DEA) to the enzyme, as implied by the photophysics, indicates that communication with the active site should in fact be feasible. Although we have not yet had any success in delivering electrons or holes to the AGAO active site employing the Re-wire, we have achieved this goal using the analogous thiol-terminated wire, as described in Chapter 6.



*References*

- (1) DiBilio, A. J.; Crane, B. R.; Wehbi, W. A.; Kiser, C. N.; Abu-Omar, M. M.; Rose, M.; Richards, J. H.; Winkler, J. R.; Gray, H. B. *J. Am. Chem. Soc.* **2001**, *123*, 3181-3182.
- (2) Wilce, M. C. J.; Dooley, D. M.; Freeman, H. C.; Guss, J. M.; Matsunami, H.; McIntire, W. S.; Ruggiero, C. E.; Tanizawa, K.; Yamaguchi, H. *Biochemistry* **1997**, *36*, 16116-16133.
- (3) Wilmot, C. M.; Murray, J. M.; Alton, G.; Parsons, M. R.; Convery, M. A.; Blakeley, V.; Corner, A. S.; Palcic, M. M.; Knowles, P. F.; McPherson, M. J.; Phillips, S. E. V. *Biochemistry* **1997**, *36*.
- (4) Larsen, R. W.; Winkler, J. R.; Chan, S. I. *J. Phys. Chem.* **1992**, *96*, 8023-8027.
- (5) Bunz, U. H. F. *Chem. Rev.* **2000**, *100*, 1605-1644.
- (6) Walters, K. A.; Ley, K. D.; Cavalaheiro, C. S. P.; Miller, S. E.; Gosztola, D.; Wasielewski, M. R.; Bussandri, A. P.; van Willigen, H.; Shanze, K. S. *J. Am. Chem. Soc.* **2001**, *123*, 8329-8342.
- (7) Marcus, R. A.; Sutin, N. *Biochim. Biophys. Acta* **1985**, *811*, 265-322.

## **Chapter 6**

### **Electrochemistry of AGAO with DEA-1-PhSH**

Our primary goal in the design of the molecular wires was to determine the redox potentials of amine oxidases, and the thiol wire was crucial in accomplishing this objective. After many trials and tribulations, the thiol terminated wire (DEA-1-PhSH (**1**), Figure 3.3) was finally synthesized and employed for electrochemical investigations of AGAO. Previous results of binding studies with the Re and benzylamine oligomer indicated that the thiol wire should also bind tightly to the enzyme. The success of this molecule for electrochemistry was dependent on its ability to bind AGAO, not only in solution, but on the electrode surface as well. A method was thus required to generate a functional protein/DEA-1-PhSH monolayer on Au.

There are several approaches to construct these “self-assembled monolayers.” The most straightforward approach involves modification of the Au electrode with the thiol molecule. The modified electrode is then placed into a solution of the protein. One concern is that this approach leads to close packing of the wires and does not leave room for subsequent binding of the bulky protein to the surface-attached molecule. Concentrations of the thiol-wire can be varied in the electrode modification, yielding different degrees of surface coverage. The distribution of the molecules on the surface will also be random, so that packing may not be an issue. The electrodes can also be prepared using a mixture of DEA-1-PhSH short chain alkyl-thiols. Addition of the second thiol-modifier allows for dispersion of the wire molecules on the Au surface and alleviates potential spatial problems for binding of the enzyme (Figure 6.1A). An additional advantage of this method is that the secondary modifiers can be selected to further enhance interaction of the protein with the electrode surface. Thus, amine-

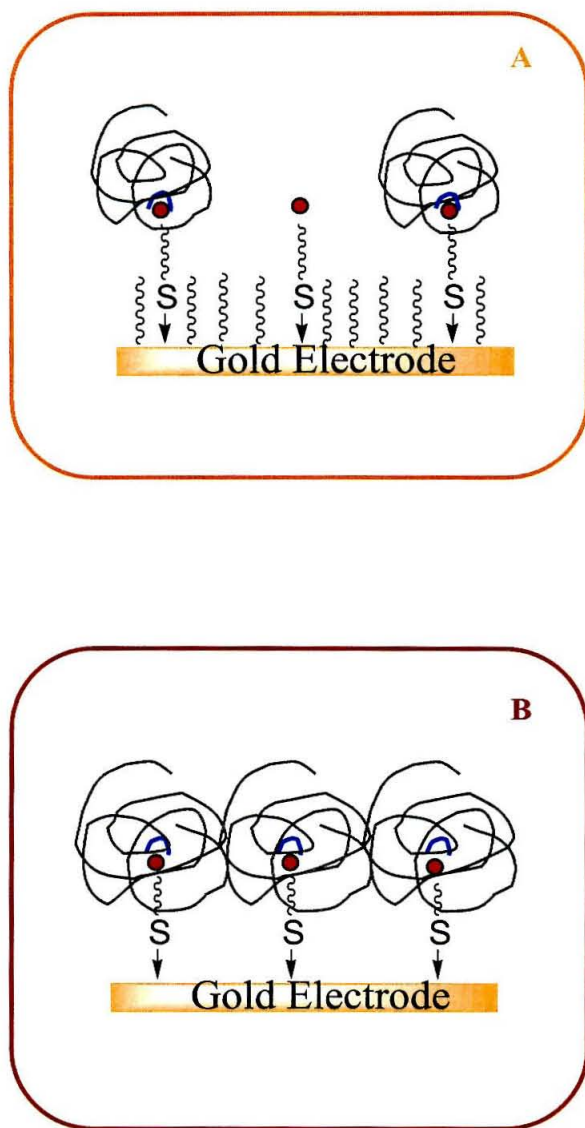


**Figure 6.1:** Depiction of self-assembled protein monolayers on gold with DEA-1-PhSH. A) The protein can also be added to an electrode surface modified with the wire alone, or a mixture of the wire and short-chain alkyl thiol modifiers. B) The wire can be pre-bound to the protein, and the AO/DEA-1-PhSH complex can then be attached to the electrode surface.

terminated short chain thiols could be employed for AGAO, which would provide favorable electrostatic interactions at the surface to aid in making a correct orientation of the protein, and promote binding to the wire monolayer.

Another option was to pre-bind the thiol wire to the protein. The resulting AGAO/DEA-1-PhSH complex can then be added to the electrode surface to construct the protein monolayer (Figure 6.1B). This method circumvents the difficulties of localizing the enzyme to the complex that are associated with the previous techniques. The thiol wire is  $\sim 22$  Å in length. By analogy to the model of Re(BzA-1-DEA) in the AGAO channel, the sulfur group of the oligomer should protrude 4.5–5 Å from the channel into solution. Thus, the protein-bound molecule should still be able to bind Au via the sulfur functionality.

We have explored several techniques in the electrochemistry of AGAO with DEA-1-PhSH. Initially, the acetyl protected wire, DEA-1-PhSAc, was synthesized and used for electrochemical studies with AGAO. Studies have indicated that thioacetyls are still able to bind to Au electrodes, though at a lower surface concentration.<sup>1</sup> Low coverage could actually help in adsorption of AGAO, for reasons described above. The complex was eventually deprotected and the electrochemistry of AGAO with DEA-1-PhSH was investigated as well.

### *Materials and Methods*

Synthesis of DEA-1-PhSAc and DEA-1-PhSH is described in Appendix B.



## *Electrochemistry*

*Apparatus and measurements:* Cyclic voltammetry (CV) and Osteryoung square-wave voltammetry (OSWV) were performed on a Bioanalytical Systems (BAS) CV50-W electrochemical analyzer. The electrochemical cell consisted of a small volume (200–300  $\mu\text{L}$ ), three-electrode, two-compartment glass cell. A Standard Calomel Electrode (SCE) served as the reference electrode and Pt wire was the auxiliary electrode. The reference compartment was separated from the working solution by a modified Luggin capillary. All solutions were deoxygenated by flowing Ar over the samples for at least 30 min.

## *Electrode preparations*

*Gold electrodes:* Commercial gold electrodes (BAS;  $A = 0.03 \text{ cm}^2$ ) were polished with 0.05  $\mu\text{m}$  alumina and sonicated for  $\sim 20$  min. They were subsequently etched in 1 M sulfuric acid by cycling from -300 mV to 1.5 V (vs. Ag/AgCl), and rinsed thoroughly with milli-Q water.

*Gold-Bead electrodes:* Gold-Bead electrodes were prepared by heating a gold wire (0.5mm diameter) slowly in a hydrogen flame, until a gold drop formed at the end of the wire. Atomic-Force Microscopy revealed these beads to be nearly completely Au(111), with flat terraces extending 50–200  $\mu\text{m}^2$ . These electrodes were etched in boiling, concentrated sulfuric acid for 30 min, then electrochemically cycled in 1 M  $\text{H}_2\text{SO}_4$  between 1.5 V and -0.3 V vs. Ag/AgCl for 30 min (scan rate = 20 mV/s). The electrodes were then sonicated for several minutes and modified.

### *Modification of Au electrodes with thiol wires and preparation of samples for electrochemistry*

*DEA-1-PhSAc*: For electrochemical studies with DEA-1-PhSAc, the complex was pre-bound to AGAO. A 1.5 mM stock solution of the wires was prepared in DMF. 20  $\mu$ L of this solution were added to 200  $\mu$ L of AGAO. AGAO concentration was  $\sim 150$   $\mu$ M, in aqueous 0.1 M  $\text{KP}_i$ , pH 7. Au electrodes were placed in this sample and soaked overnight at 4°C to allow formation of the protein/wire monolayer. Electrodes were also placed in a similar solution containing only the thiol at identical concentrations, without AGAO, as the control.

*DEA-1-PhSH*: Stock solutions of DEA-1-PhSH were prepared in MeOH/ $\text{CH}_3\text{CN}$  (2:1), at mM concentrations. Solutions were kept under Ar to prohibit disulfide formation. Protein-bound wire samples were prepared by adding  $\sim 10$   $\mu$ L of this solution to 100  $\mu$ L of AGAO. Gold Balls were modified 1) by soaking the electrodes in the protein/wire solution overnight at 4°C or 2) by first soaking electrodes overnight in the stock DEA-1-PhSH solution, and subsequently soaking in protein solution overnight at 4°C. AGAO concentration was 100  $\mu$ M in 50 mM HEPES buffer, pH 7.

### *Determination of thiol coverage on Au electrodes*

Gold-bead electrodes modified with DEA-1-PhSH were reductively stripped in 1 M KOH to determine the amount of thiol bound to the surface.

### *Electrochemistry with DEA-1-PhSAc*

#### *Results*

Electrochemistry of AGAO was investigated with DEA-1-PhSAc by pre-binding of the molecule to the protein at a 1:1 ratio of AO:thiol-wire, followed by modification

of the electrodes with the protein/wire solution. A redox wave was observed by square wave voltammetry, at -365 mV vs. SCE (Figure 6.2A). The electrode was subsequently removed from the protein solution and placed into buffer. The resulting scan showed a significantly diminished signal at the above potential (Figure 6.2B). Placement of the electrode back into the protein sample restored the redox wave (Figure 6.2C). SWV of a DEA-1-BzA modified Au electrode, prepared in the absence of protein, was also examined in  $\text{KP}_i$ . Scanning from 0 to -500 mV did not produce a redox wave for this electrode.

### *Discussion*

Electrochemical experiments with DEA-1-PhSAc demonstrate a redox couple centered at -365 mV vs. SCE. This potential accords well with the potentials observed in our initial studies of the amine oxidase electrochemistry (see Chapter 2). The potential was thus presumed to be due to the TPQ cofactor of AO. When the electrode was removed from the protein sample and placed into buffer, the redox wave was barely discernible. This behavior implied that AGAO bound to the surface of the electrode diffused from the monolayer into the buffer solution. Once the electrode was returned to the protein solution, the redox couple was again apparent. This is consistent with re-adsorption of AGAO onto the electrode surface. These results provided further evidence that the potential was due to protein. The redox couple was not seen by square wave voltammetry on electrodes modified solely with DEA-1-PhSAc, so that a redox couple due to the thiol oligomer itself was excluded as a possible explanation.

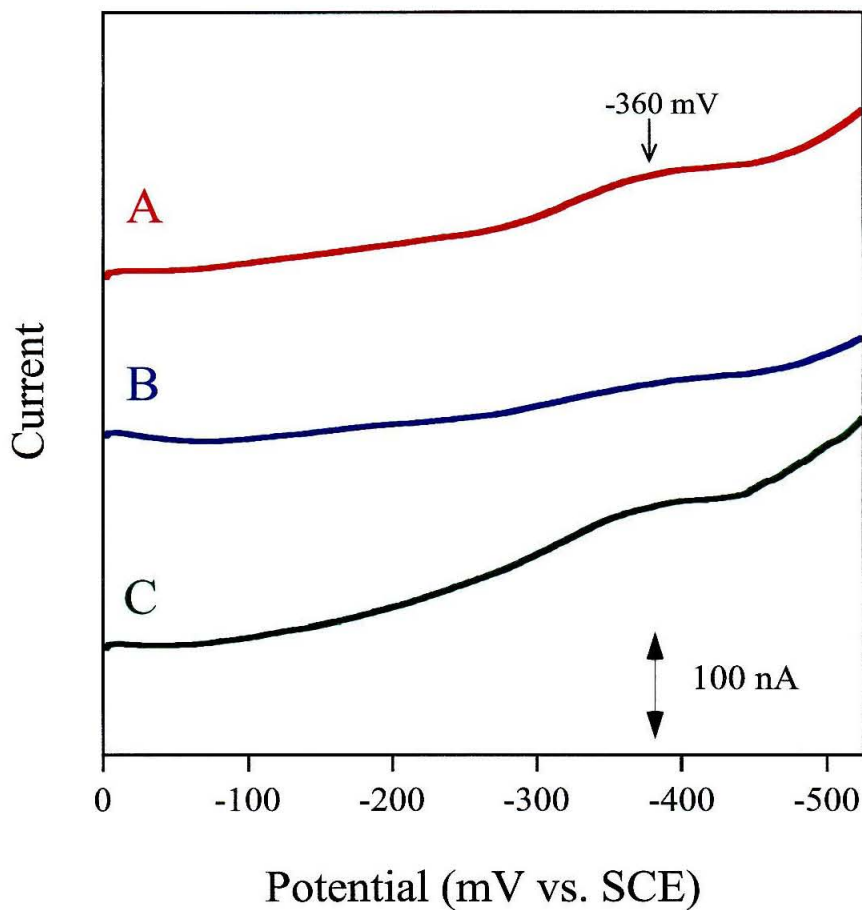


**Figure 6.2:** Electrochemistry of AGAO with DEA-1-PhSAC

A) Results for electrochemistry of gold electrode soaked in 1:1 thiol : AGAO solution for 36 h.

B) Voltammogram after removing electrode from the protein solution, and placement into  $\text{KP}_i$ .

C) Voltammogram after electrode is placed back into the protein/thiol wire solution.

Samples in aqueous 0.1 M  $\text{KP}_i$ , pH 7.



The amplitude of the redox signals observed by SWV was smaller than we had hoped. We attribute this to the reduced ability of the acetyl-protected thiol wire to bind to the electrode, compared to the free thiol. Although modification of Au electrodes by thioacetyl molecules has been reported<sup>1</sup>, the mechanism by which the thioacetyls bind to Au is unclear. It was speculated that the acetyl group is liberated upon adsorption to the Au surface. However, slower rates of monolayer formation are observed and much higher concentrations of the protected thiol compounds are required. The free sulfhydryl group forms much stronger bonds to Au. Methods previously described for in situ deprotection and electrode modification were unsuccessful<sup>3</sup>. The procedure did not afford the free thiol (as determined by mass spectroscopy), nor was binding of the complex to the electrode observed. Therefore, DEA-1-PhSAc was deprotected, DEA-1-PhSH was isolated, and the electrochemistry of this wire was investigated with AGAO.

### *Electrochemistry with DEA-1-PhSH*

#### *Results*

The electrochemistry of AGAO was carried out using gold electrodes modified with the protein-bound thiol. The initial experiment was carried out in the presence of dioxygen. CV revealed an irreversible reduction at -350 mV vs. SCE, characteristic of a catalytic current (Figure 6.3). This signal disappeared upon degassing, and reappeared with the addition of O<sub>2</sub>. As a control, the electrochemistry of a DEA-1-PhSH modified electrode was also examined. The reduction at -350 mV was not observed in the control.

The electrochemistry of AGAO was also investigated using DEA-1-PhSH modified Au electrodes, which had been placed into protein solution overnight. OSWV



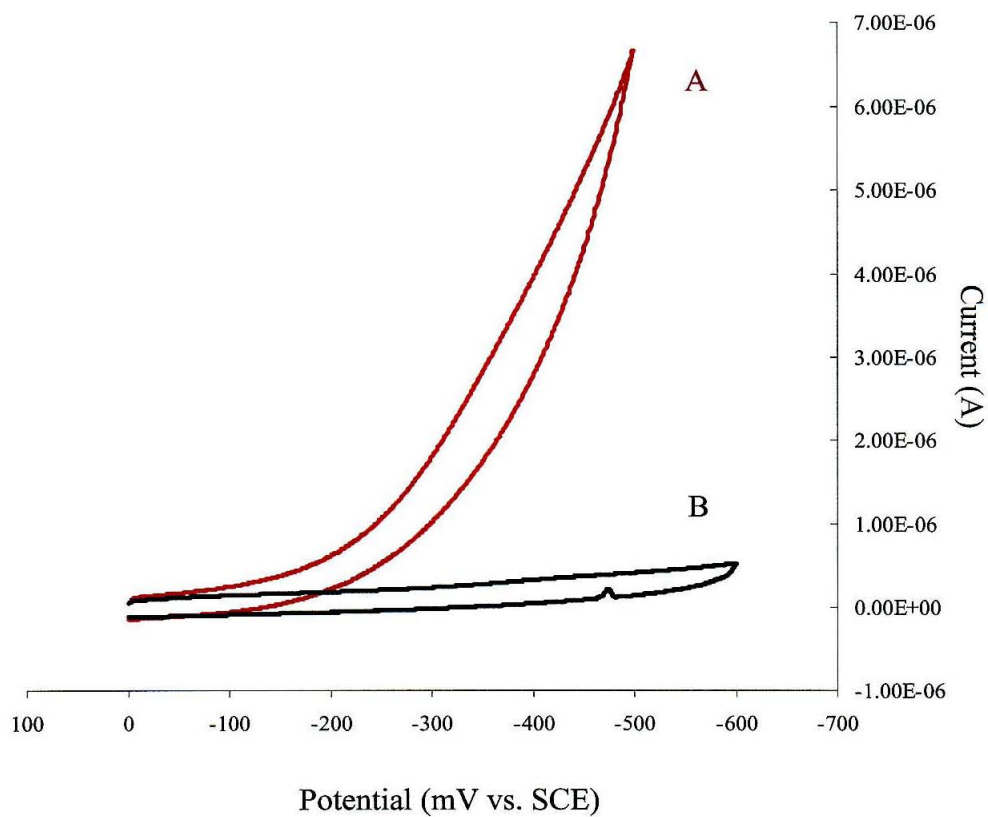


**Figure 6.3:** Cyclic voltammetry of AGAO on Au electrodes modified by 1<sup>st</sup> method, with DEA-1-PhSH/AGAO solution: **A)** oxygenated sample; **B)** deoxygenated sample. Scans in 50 mM HEPES buffer, pH 7. Scan rate = 25 mV/s.

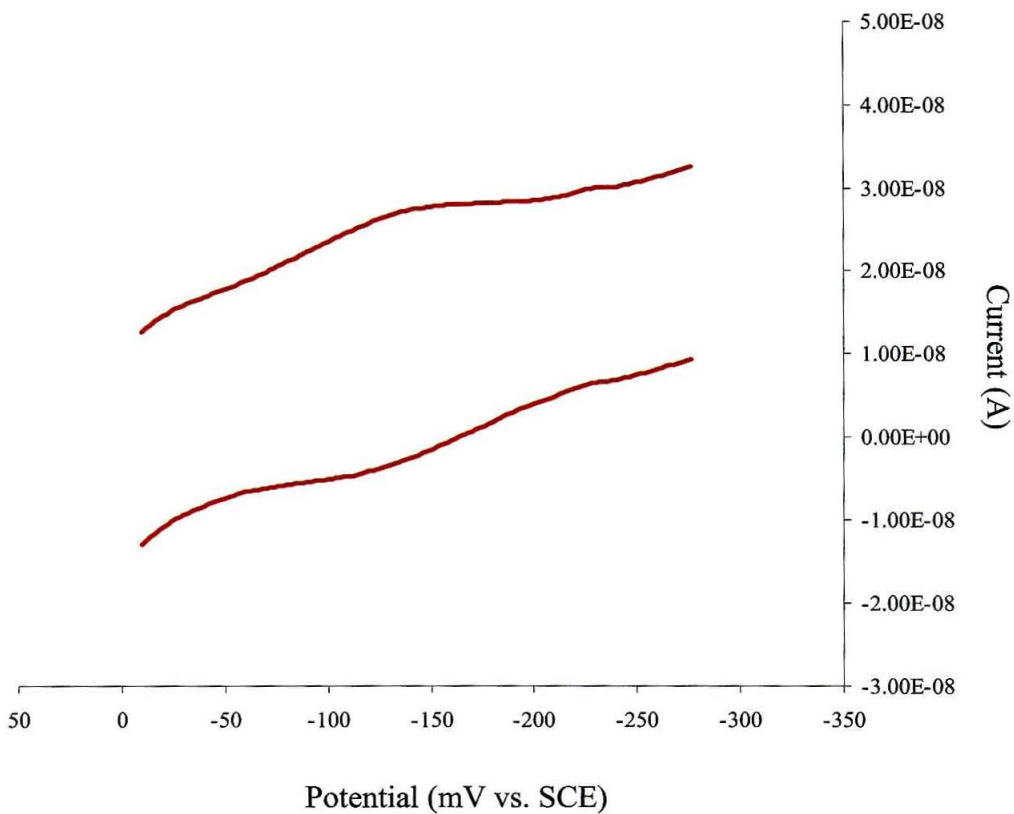


**Figure 6.4:** OSWV of AGAO on DEA-1-PhSH modified Au electrodes.  $E^{1/2} = -130$  mV vs. SCE. [AGAO] = 100  $\mu$ M in 50 mM HEPES, pH 7. Sweep Amplitude: 15 mV; sweep frequency: 5 Hz; potential step: 2 mV.

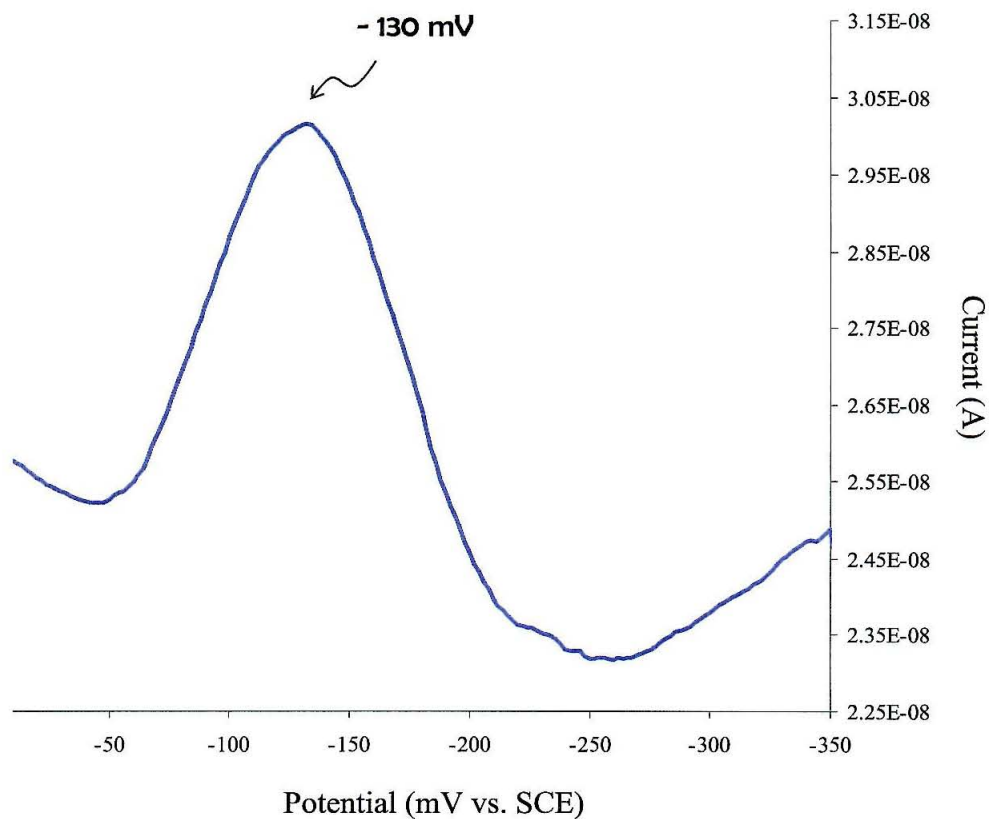


**Figure 6.5:** Difference spectrum for OSWV of AGAO on DEA-1-PhSH modified Au electrodes. [AGAO] = 100  $\mu$ M in 50 mM HEPES, pH 7. Sweep Amplitude: 15 mV; sweep frequency: 5 Hz; potential step: 2 mV.

of a deoxygenated protein sample exhibited a reversible redox couple centered at -130 mV vs. SCE (Figure 6.4, 6.5). Introduction of dioxygen to this solution did not produce the catalytic current observed for the DEA-1-PhSH/AGAO modified electrodes. The CV for the thiol-only modified electrode in  $KP_i$  did not display a redox wave in this region.

### *Discussion*

The electrochemistry resulting from electrodes modified with DEA-1-PhSH pre-bound to AGAO demonstrated a large catalytic current that we attribute to protein-induced  $O_2$  reduction. The aminoquinol, generated by reduction of TPQ with the amine substrate, reacts rapidly with  $O_2$ . The electrochemically reduced topaquinone is thus expected to catalytically reduce dioxygen as well. Upon degassing of the solution, however, the catalytic wave disappears. A redox wave at  $\sim -400$  mV was barely discernible by OSWV. These results can be explained as due to nonspecific adsorption of the protein onto the electrode surface. This could be a result of the method used for preparation of the thiol/protein monolayer, which involves soaking the electrodes in the protein solution. The technique may not permit formation of an ideal wire/AGAO surface, as depicted in Figure 6.1A. The protein may instead be adsorbed onto the surface in an unfavorable conformation in which the active site is also accessible to  $O_2$ . The minute signal seen in the deoxygenated solutions could be due to the small quantity of AGAO on the surface. KOH stripping experiments on the gold monolayer surface provide further evidence for this conclusion. These experiments demonstrate that only trace amounts of DEA-1-PhSH are bound to the electrode surface.

In contrast, the results of electrochemical studies with electrodes in which the protein is added to DEA-1-PhSH modified Au electrodes indicate a very different surface monolayer. OSWV of AGAO reveals a reversible redox couple at -130 mV vs. SCE, which we attribute to TPQ. Introduction of dioxygen to the sample does not lead to catalytic reduction observed in the previous experiments. This suggests that the AGAO active site on the thiol-wire monolayer is no longer accessible to O<sub>2</sub>. We conclude that the monolayer formed by this technique is much like that depicted in Figure 6.1B, in which the protein is complexed to bound thiol wires on the Au surface. KOH stripping experiments also indicate much better DEA-1-PhSH surface coverage for electrodes prepared by this method. Stripping coulometry indicates roughly 73% ( $\pm$  20%) surface coverage on the Au-bead electrodes. The AGAO potential obtained in these experiments is shifted to more positive values, but is now completely reversible. This is further evidence of the two different protein environments generated by these two methods. The more negative, irreversible redox couple previously observed is likely due to adsorbed protein that may also be slightly denatured.

The redox potential of -130 mV vs. SCE agrees well with the potential obtained from electrochemical studies of topaquinone model complexes<sup>4</sup>. We thus conclude that the potential displayed in these studies is due to the TPQ cofactor of AGAO. Importantly, we have demonstrated that the designed molecular wires can in fact bind amine oxidase and establish communication with the active site. These complexes therefore open new avenues for future studies of amine oxidases; and they also may provide a means to access buried redox sites in other enzymes.



*References*

- (1) Tour, J. M.; Jones II, L.; Pearson, D. L.; Lamba, J. J. S.; Burgin, T. P.; Whitesides, G. W.; Allara, D. L.; Parikh, A. N.; Atre, S. V. *J. Am. Chem. Soc.* **1995**, *117*, 9529-9534.
- (2) Preparaton of Gold-Bead electrodes and KOH stripping experiments were carried out with the assistance of Ryutaro Tanimura, a graduate student with Dr. Katsumi Niki, at Occidental College.
- (3) Yu, C. J.; Chong, Y.; Kayyem, J. F.; Gozin, M. *J. Org. Chem* **1999**, *64*, 2070-2079.
- (4) Mure, M.; Klinman, J. P. *J. Am. Chem. Soc.* **1993**, *115*, 7117-7127.

## **Appendix A**

### **Protein purification and sample preparation**

### *Protein expression and purification*

Samples of purified amine oxidase were obtained from D. M. Dooley and his group at Montana State University. The copper amine oxidase from *Arthrobacter globiformis* was expressed and purified as a fusion protein with a C-terminal *Strep*-tag II peptide. The procedures for expression and isolation of AGAO are described by Juda et al.<sup>1</sup>.

### *AGAO sample preparation*

Protein samples were used as received. When necessary, AGAO samples in HEPES buffer were exchanged into phosphate buffer by dialysis against a 1000-fold volume of 0.1 M KPi, pH 7 (30 kDa molecular weight cutoff dialysis tubing; changing buffer every 8 hours), for 16 hours. Samples were concentrated using a Millipore Ultrafree-15 centrifugal filter (10 kDa molecular weight cutoff). AGAO concentrations were determined from the absorbance at 280 nm ( $\epsilon_{280} = 1.32 \text{ mg/mL}$ ) or from the TPQ absorbance at 480 nm ( $\epsilon = 2500 \text{ M}^{-1} \text{ cm}^{-1}$  per TPQ). Specific activities of the protein were determined by means of an assay for  $\text{H}_2\text{O}_2$  production, coupled to the oxidation of 2,2'-azinobis(3-ethylbenzthiazoline-6-sulfonic acid) by horseradish peroxidase, using phenethylamine as the substrate, as previously described<sup>2</sup>. Specific activity is described as micromoles of product per minute per milligram, and ranged from 19–22 units/mg for the AGAO samples received. Protein samples were stored at  $-80^\circ\text{C}$  until use.

*References*

- (1) Juda, G. A.; Bollinger, J. A.; Dooley, D. M. *Protein Expression and Purification* **2001**, 22, 455-461.
- (2) Stutowicz, A.; Kobes, R. D.; Orsulak, P. J. *Anal. Biochem.* **1984**, 138, 86-94.

## **Appendix B**

### **Synthesis and characterization of molecular wires**



### *General*

Aryl halides, TMS-acetylene, Pd and Cu catalysts were obtained from commercial sources. Fluka “puriss” diethylamine, diisopropylamine and THF were used in the Pd coupling reactions. HPLC grade solvents were used for mass spectrometry. Deuterated solvents were purchased from Cambridge Isotope Laboratories or Aldrich. All other solvents were reagent grade. The  $(\text{phen})\text{Re}^{\text{I}}(\text{CO})_3(\text{OH}_2)]^{\text{TF-}}$  starting complex was synthesized by William Wehbi, according to procedures described by Sullivan and Meyer<sup>1</sup>. Compounds were generally purified by flash chromatography<sup>2</sup> on EM Science silica gel (230–400 mesh).

Gas chromatography/mass spectrometry (GC-MS) was recorded on an Agilent Technologies instrument. Electrospray mass spectrometry (ES-MS) and atmospheric pressure chemical ionization (APCI) were performed on a Hewlett Packard 1100 series instrument, at the Environmental Analysis Center at Caltech.

### *General procedures for Pd cross-coupling reactions*

The scheme for synthesis of the molecular wires is outlined in Figures **B.1** and **B.2**. The molecules were synthesized by Pd catalyzed cross-coupling reactions. The general procedure is as follows: The aryl halide and acetylene terminated compound were placed in a pressure tube containing ~ 20–30 mL of solvent and the solution was degassed by bubbling with Ar for 20 min. (trimethylsilylacetylene, TMS-acetylene, was added in the final step, in reactions using this reagent).  $(\text{Ph}_3\text{P})_2\text{Pd}^{\text{II}}\text{Cl}_2$  (2%) and CuI (0.5%) were added to the solution, and the mixture was degassed for several more min.

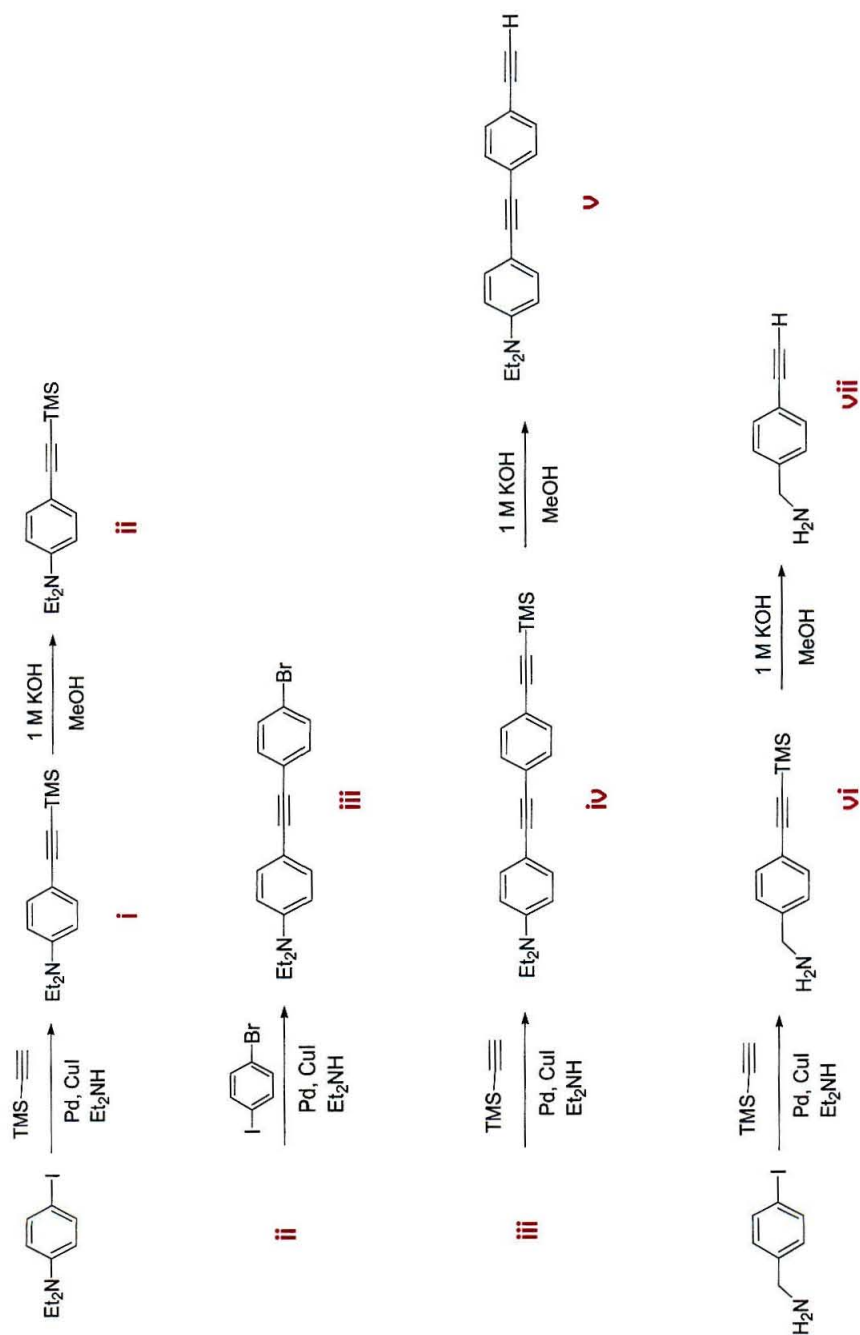


**Figure B.1:** Synthesis scheme for molecular wire precursors.

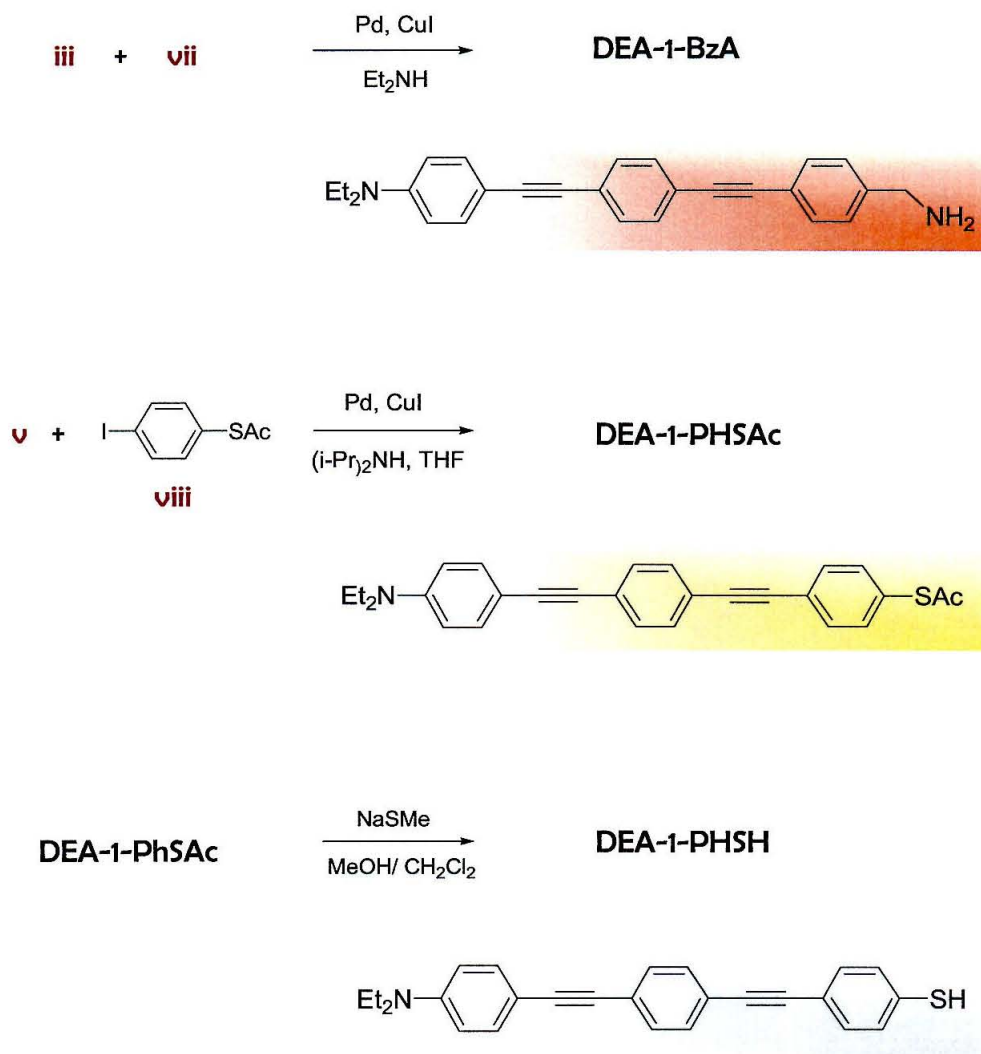


**Figure B.2:** Scheme for synthesis of molecular wires.

The pressure tube was capped, and the reaction mixture was sonicated for 12 hours. The solvent was removed *in vacuo* and the product purified by column chromatography. Specific details for the synthesis and purification of each molecule, and their characterization by MS and NMR are given below.

### *Synthesis and Purification of oligomers*

**Et<sub>2</sub>NPh≡-TMS (i):** In a typical reaction, 0.5 g of p-iododiethylaniline (1.8 mmol), 0.4 mL TMS-acetylene (2.4 mmol; 1.3 eq.), 20 mL Et<sub>2</sub>NH, 2% Pd and 0.5% CuI were combined in a pressure tube, and sonicated as described above. Product was purified by column chromatography using 1:2 CH<sub>2</sub>Cl<sub>2</sub>/hexane, R<sub>f</sub> = 0.x; 69% yield. GC-MS: m/e = 245, t = 12 min. (p-bromodiethylaniline could also be used in place of p-iododiethylaniline, however, the reaction typically required several additions of Pd, Cu and TMS-acetylene).

**Et<sub>2</sub>NPh≡-H (ii):** 1 eq. of 1 M KOH was added to X in 250 mL MeOH, and stirred for ~ 12 hours. MeOH was removed and the product was extracted with ether. The organic layer was dried with MgSO<sub>4</sub>, filtered and the solvent removed *in vacuo*, to afford **ii** in 66% yield. <sup>1</sup>H NMR (300 MHz, CDCl<sub>3</sub>): δ 1.15 (t, 6H) 3.34 (q, 4H) 2.94 (s, 1H) 6.55 (d, 2 H), 7.31 (d, 2 H) GC-MS: m/e = 173, t = 10 min.

**Et<sub>2</sub>NPh≡-PhBr (iii):** One equivalent of iodobromobenzene was added to a solution of **ii** in Et<sub>2</sub>NH, along with 2% Pd and 0.5% CuI. Product was purified by column chromatography using 3:7 CH<sub>2</sub>Cl<sub>2</sub>/hexane, R<sub>f</sub> = 0.35; 95% Yield. <sup>1</sup>H NMR (300 MHz, CDCl<sub>3</sub>, Figure B.3) δ 1.15 (t, 6H) 3.35 (q, 4H), 6.58 (d, 2H), 7.32 (m, 4 H), 7.41 (d, 2H) GC-MS: m/e = 328, t = 16 min.

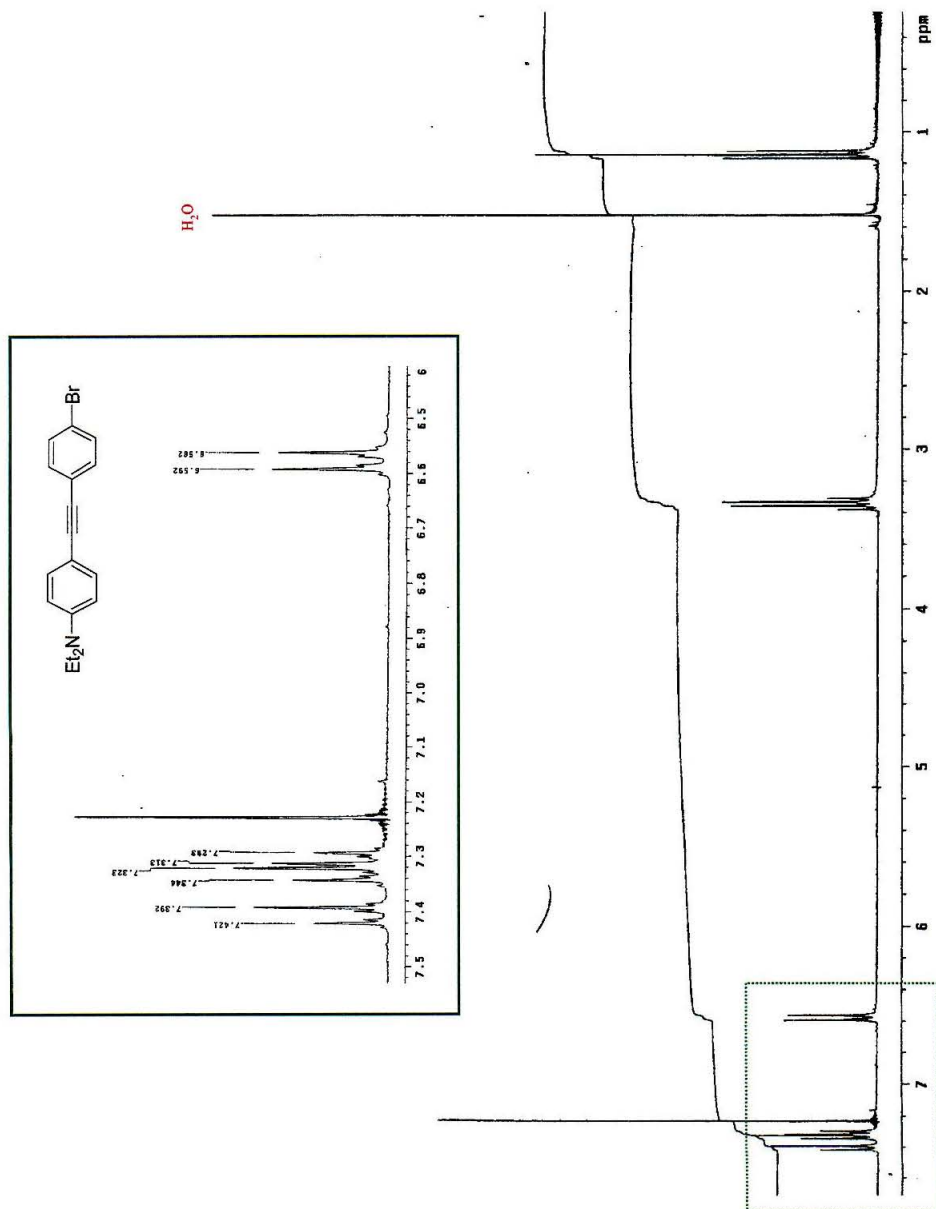


Figure B.3:  $^1\text{H}$  NMR of **iii** in  $\text{CDCl}_3$ . Inset: aromatic region magnified.



**H<sub>2</sub>NH<sub>2</sub>CPh≡TMS (vi):** Conditions for the reaction of p-iodo or p-bromobenzylamine with TMS-acetylene were analogous to those described for **i**. Product was purified by column chromatography using 85% CH<sub>2</sub>Cl<sub>2</sub>/15% MeOH, R<sub>f</sub> = 0.3; 78 % Yield. GC-MS: m/e = 203, t = 9.6 min.

**H<sub>2</sub>NH<sub>2</sub>CPh≡H (vii):** Deprotection of **vi** was carried out according to procedures for synthesis of **ii**. The work-up procedures were also identical. Yield = 40%. <sup>1</sup>H NMR (300 MHz, dmf-d<sub>6</sub>, Figure **B.4**): δ 3.81 (s, 1H) 4.08 (s, 2H) 7.4 (d, 2 H), 7.46 (d, 2 H) GC-MS: m/e = 131, t = 8.4 min.

**DEA-1-BzA:** In a typical reaction, 0.56 g of **iii** (1.7 mmol) and 0.23 g of **vii** (1.7 mmol; 1 eq.) were added to 50 mL of Et<sub>2</sub>NH. 2% Pd, and 0.5% CuI were used. The crude product was evaporated onto alumina, and the solid was loaded onto a column of silica gel. Product was eluted using an 85% CH<sub>2</sub>Cl<sub>2</sub>/15% MeOH mixture, R<sub>f</sub> = 0.25; 87% Yield. <sup>1</sup>H NMR (300 MHz, dmf-d<sub>6</sub>, Figure **B.5**): δ 1.15 (t, 6H) 3.45 (q, 4H) 4.01 (s, 2H) 6.76 (d, 2 H), 7.41 (d, 2 H) 7.58 (m, 8H) <sup>13</sup>C NMR (500 MHz, dmf-d<sub>6</sub>): δ 12, 44.2, 45.1, 87.11, 88.22, 91.29, 93.84, 108, 111.65, 121.52, 122.2, 124.55, 128.45, 131.45, 131.77, 131.95, 133.3, 142.7, 148.34 ES-MS: [m+1] = 379

**Et<sub>2</sub>NPh≡Ph≡TMS (iv):** TMS-acetylene was coupled to **iii** by procedures described for **i**. Product was purified by column chromatography using 4:6 CH<sub>2</sub>Cl<sub>2</sub>/hexane, R<sub>f</sub> = 0.4; 83% Yield. <sup>1</sup>H NMR (300 MHz, CD<sub>2</sub>Cl<sub>2</sub>): δ 0.24 (s) 1.15 (t, 6H) 3.34 (q, 4H) 2.94 (s, 1H) 6.62 (d, 2 H), 7.34 (d, 2 H) 7.4 (s, 4 H) GC-MS: m/e = 345, t = 17 min.

**Et<sub>2</sub>NPh≡Ph≡H (v):** **iv** was deprotected by procedures described for **ii**. After extraction with ether, no further purification was generally required. Yield = 86%. GC-MS: m/e = 273, t = 15.4 min.



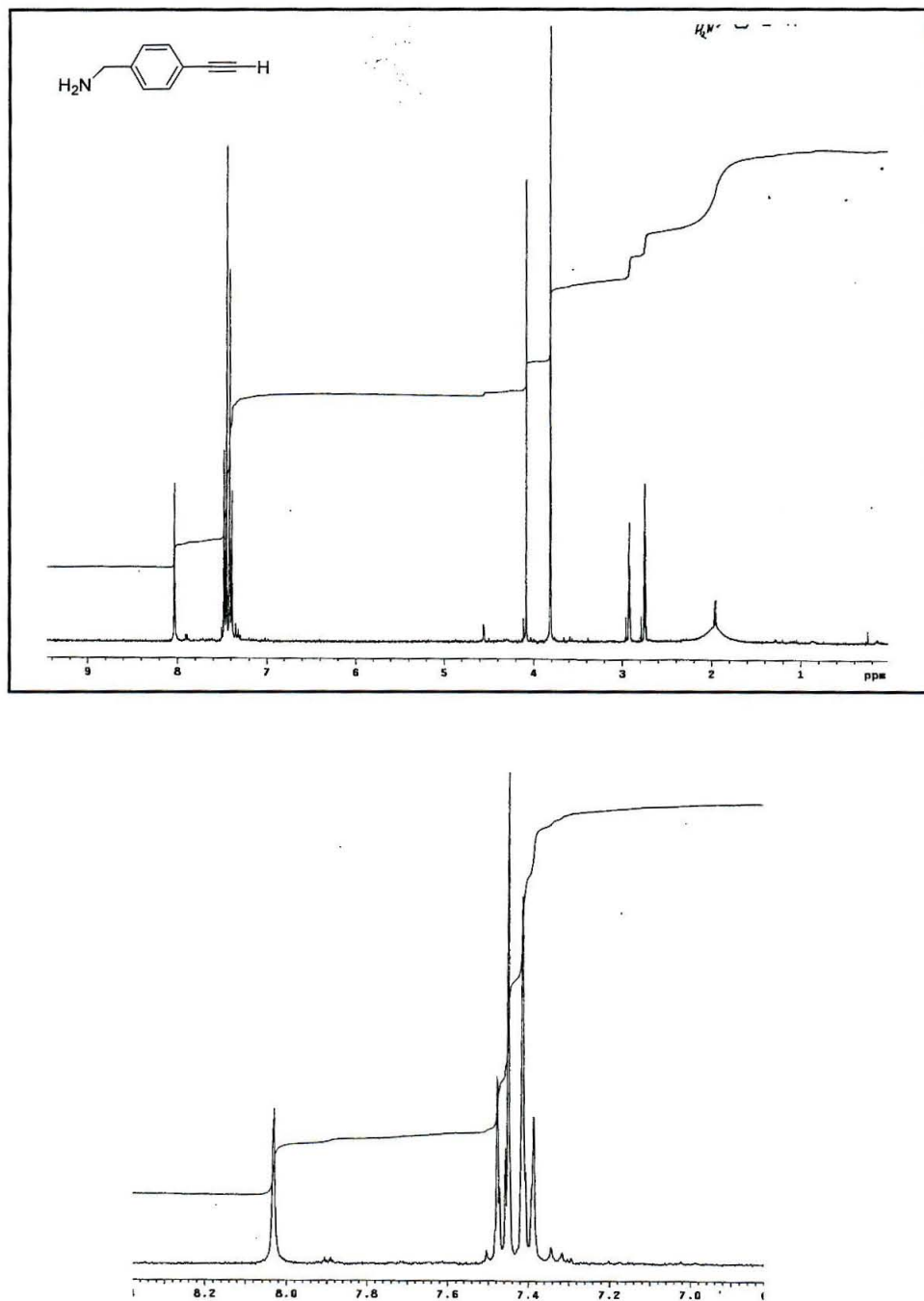


**Figure B.4:**  $^1\text{H}$  NMR of **vi** in  $\text{dmf-d}_6$ . Bottom: aromatic region magnified.

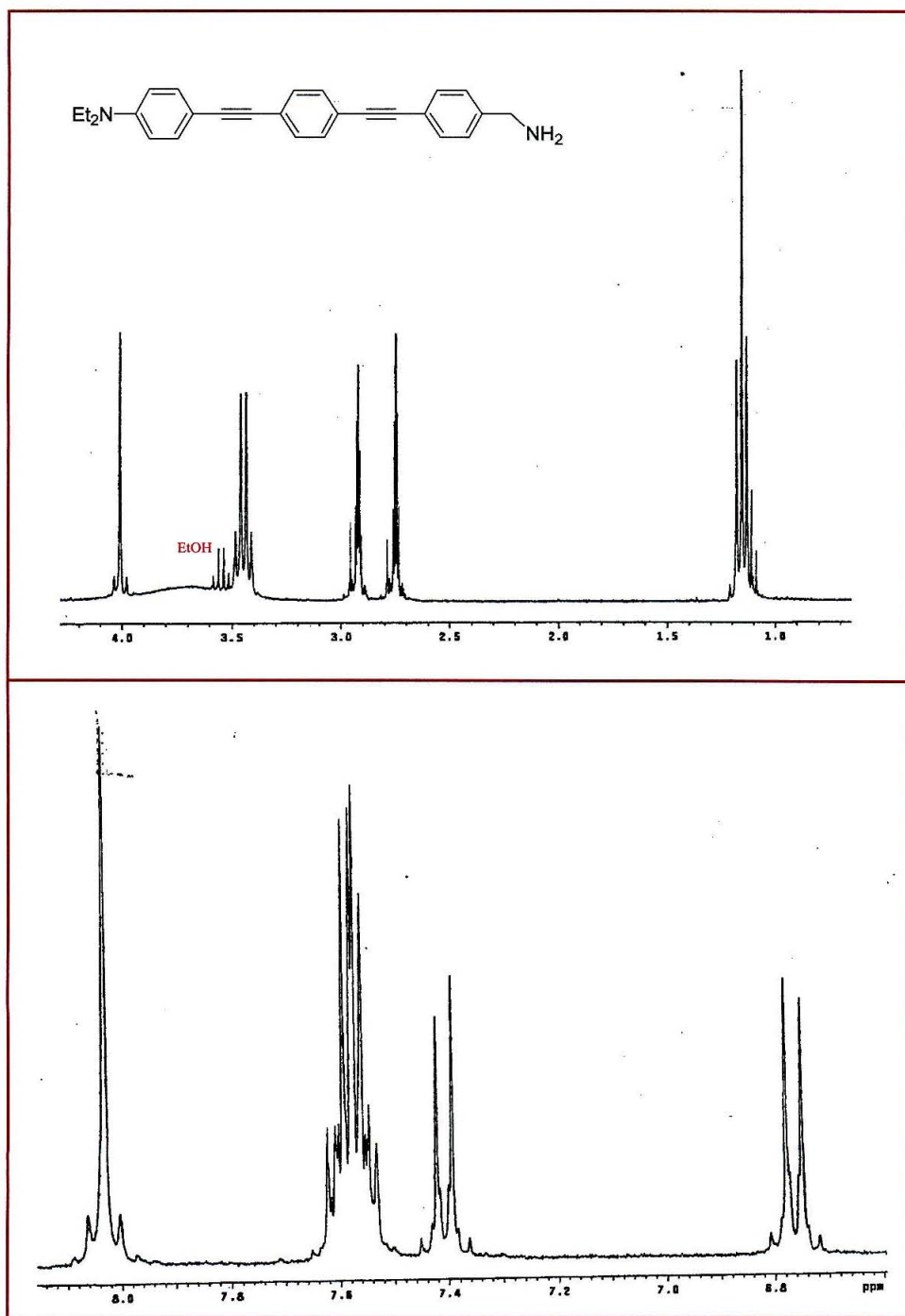


**Figure B.5:**  $^1\text{H}$  NMR of DEA-1-BzA in  $\text{dmf-d}_6$ . Top: alkyl region magnified. Bottom: aromatic region magnified.

**I-Ph-SAc (viii):** The acetyl protected thiophenol was synthesized by modification of procedures previously described<sup>3</sup>. To a solution of 5 g of diiodobenzene (15 mmol) ether (15 mL) at -78°C was added dropwise 17.7 mL of *t*-BuLi (1.7M solution in pentane, 30 mmol) under Ar. The solution was stirred at -78°C for 30 min., and then warmed to 0°C for 15 min. The solution was then re-cooled to -78°C and a suspension of 0.55g of sulfur powder (2.14 mmol) in 40 mL THF was added. The mixture was stirred for 15 min. at -78°C and warmed to 0°C for 30 min. After re-cooling to -78°C again, 1.9 mL of acetyl chloride (27 mmol) was added. The reaction was allowed to warm to room temperature overnight. The mixture was extracted with CH<sub>2</sub>Cl<sub>2</sub>, the organic layer collected and the solvent removed in vacuo. The product was then purified by column chromatography using 2:1 hexane/CH<sub>2</sub>Cl<sub>2</sub>. *R*<sub>f</sub> = 0.25; 67% yield <sup>1</sup>H NMR (300 MHz, CDCl<sub>3</sub>): δ 2.41 (s, 3H) 7.11 (d, 2 H), 7.72 (d, 2 H) GC-MS: *m/e* = 278, *t* = 11 min.

**DEA-1-PhSAc:** 0.273 g **v** (.28 mmol) and 0.278 g **viii** (.28 mmol; 1 eq) were dissolved in 16 mL of a 1:1 mixture of THF/di-isopropylamine. 2% Pd and 5.5% CuI were added. The product was purified by column chromatography using 4:6 CH<sub>2</sub>Cl<sub>2</sub>/Hexane, *R*<sub>f</sub> = 0.2; 63% yield. <sup>1</sup>H NMR (300 MHz, CD<sub>2</sub>Cl<sub>6</sub>, Figure **B.6**, **B.7**): δ 1.15 (t, 6H) 3.45 (q, 4H) 4.01 (s, 2H) 6.55 (d, 2 H), 7.2 (d, 2 H), 7.27 (d, 2H), 7.36 (d, 2H), 7.41 (q, 4H), 7.48 (d, 2H) ES-MS, APCI: [*m*+1] = 424.

**DEA-1-PhSH:** The deprotection of DEA-1-PhSAc was according to procedures previously described for deprotection of thioacetyls<sup>4</sup> with the exception that the oligomer was dissolved in MeOH/CH<sub>2</sub>Cl<sub>2</sub> (enough CH<sub>2</sub>Cl<sub>2</sub> was added to dissolve the compound completely). The reaction was allowed to proceed for ~ 45 min. Extraction was carried out as described. ES-MS: [*m*+1] = 381

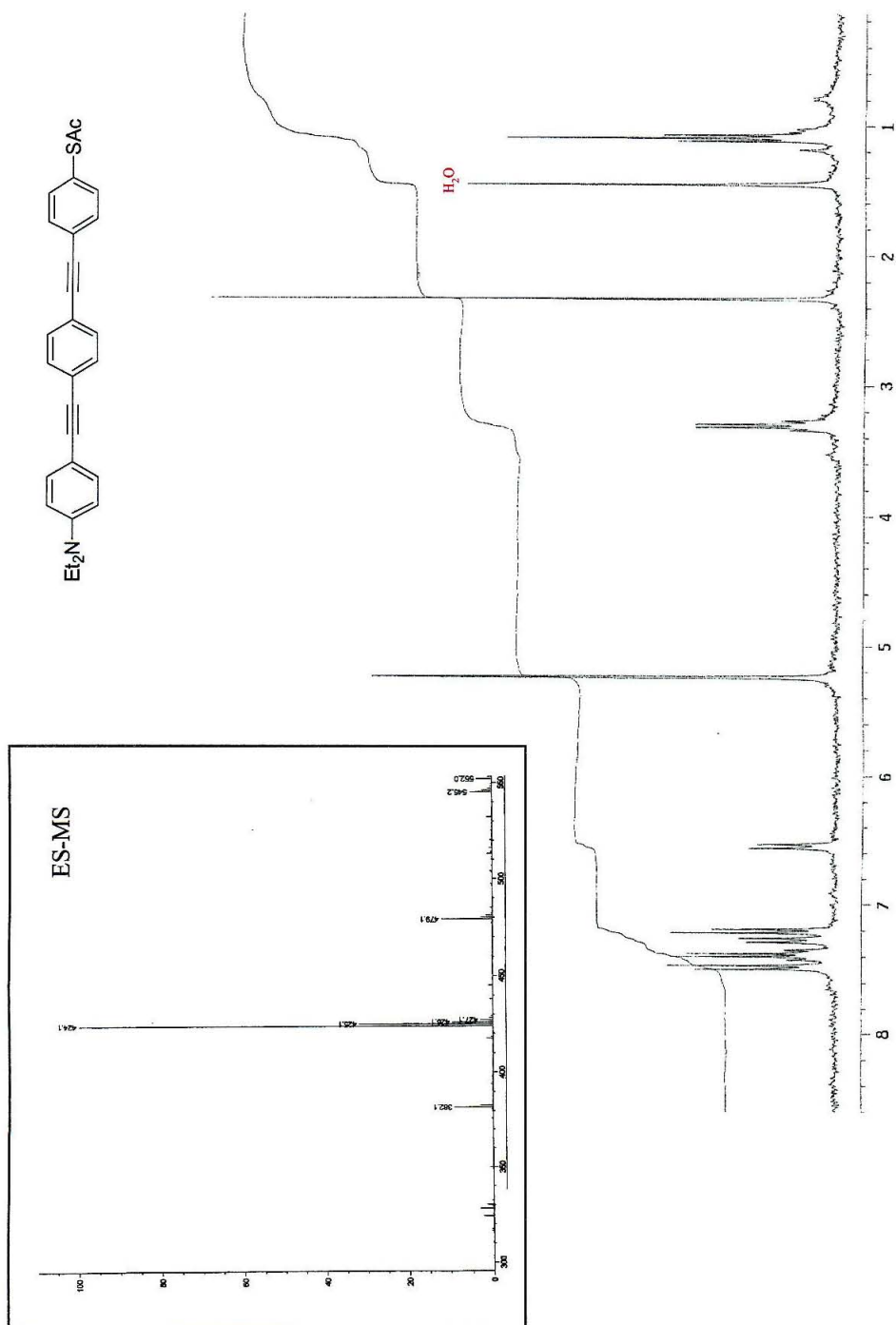


**Figure B.6:**  $^1\text{H}$  NMR of DEA-1-PhSAc in  $\text{CD}_2\text{Cl}_2$ . Inset: ES-MS,  $[m+1] = 424$ .

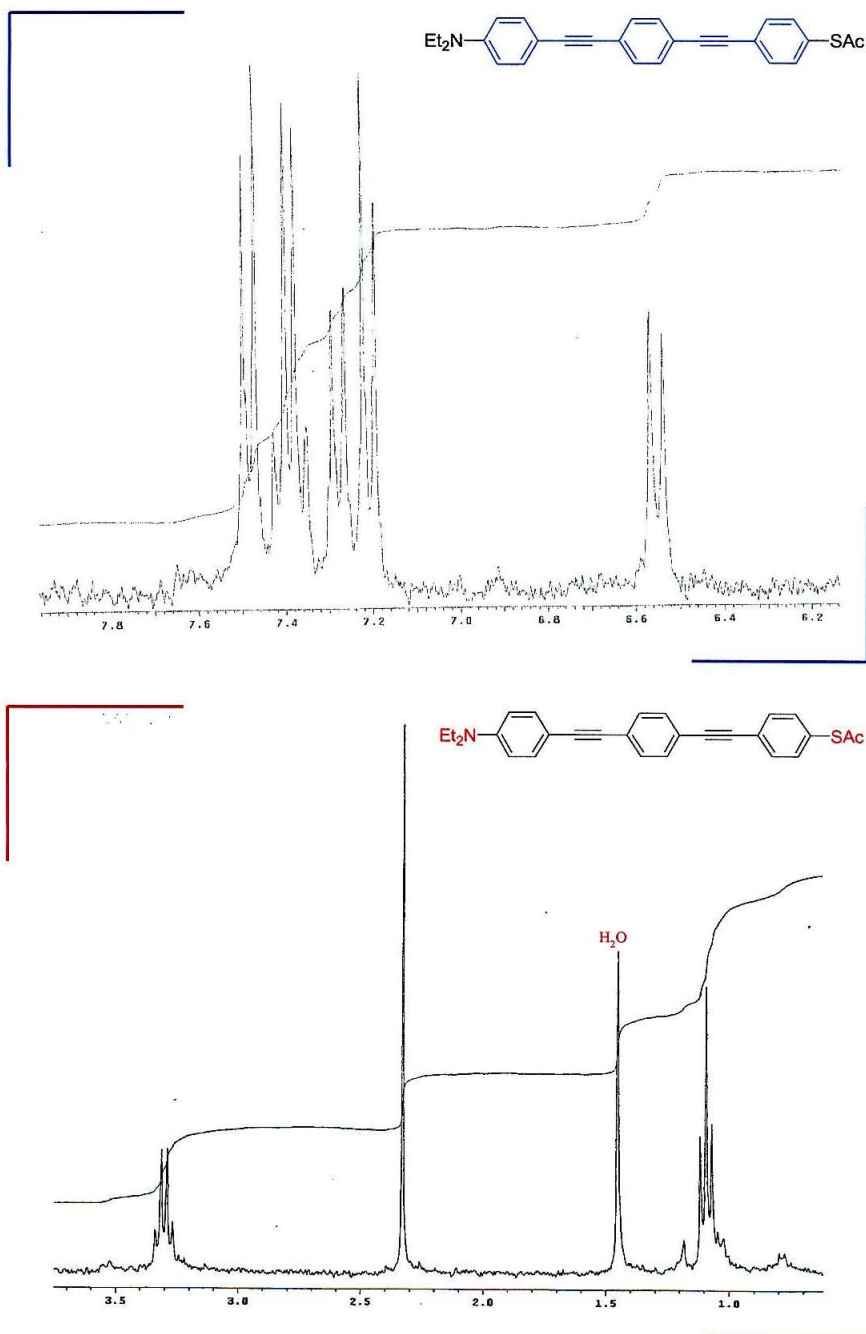


**Figure B.7:**  $^1\text{H}$  NMR of DEA-1-BzA in  $\text{CD}_2\text{Cl}_2$ . Top: aromatic region magnified. Bottom: alkyl region magnified.

*Synthesis of Re(BzA-1-DEA)*

**$[(\text{phen})(\text{CO})_3\text{Re}^{\text{I}}(\text{BzA-1-DEA})]^{\text{Tf}^-}$**  ( $\text{X} = \text{Re}(\text{BzA-1-DEA})$ ):  $(\text{phen})\text{Re}(\text{CO})_3(\text{OH}_2)^{\text{Tf}^-}$  (0.05g, 0.2 mmol) and DEA-1-BzA (0.1g, 0.26 mmol), were dissolved in 20 mL of MeOH and 10 mL of  $\text{CH}_2\text{Cl}_2$  (the mixture is required to dissolve the oligomer). The reaction was refluxed for 1 week at 60–70°C. The progress of the reaction was monitored by ES-MS ( $(\text{phen})(\text{CO})_3\text{Re}^{\text{I}}$ :  $[m+1] = 451$ ; DEA-1-BzA:  $[m+1] = 379$ ;  $\text{Re}(\text{BzA-1-DEA})$ :  $[m+1] = 829$ ). The product mixture was purified by flash chromatography on silica gel using a mixture of THF/MeOH, 2:1, containing 5% triethylamine (TEA) to elute all unwanted products and starting materials. The desired Re complex was then eluted with THF/MeOH containing 5% TEA and 2% saturated  $\text{KNO}_3$ . The solvent was removed under vacuum, and the product was washed thoroughly with water to remove any  $\text{KNO}_3$  present. The product was dried under vacuum overnight.  $^1\text{H}$  NMR is shown in Figure **B.8** (300 MHz,  $\text{CD}_3\text{CN}$ ),  $^1\text{H}$  NMR of  $(\text{phen})\text{Re}^{\text{I}}(\text{CO})_3(\text{OH}_2)^{\text{Tf}^-}$  is shown in Figure **B.9** for comparison.



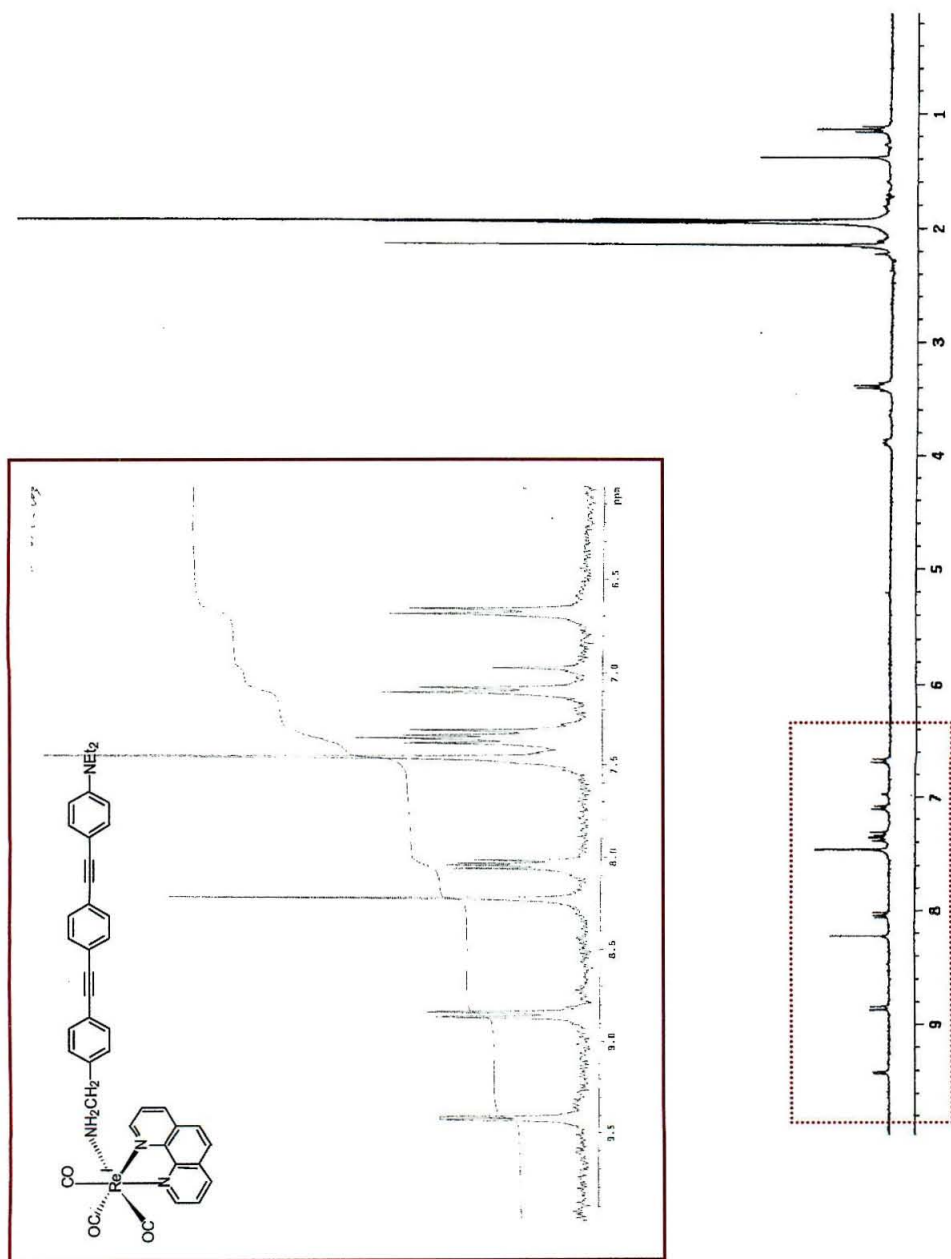


**Figure B.8:**  $^1\text{H}$  NMR of  $\text{Re}(\text{BzA-1-DEA})$  in  $\text{CD}_3\text{CN}$ . Inset: aromatic region magnified.

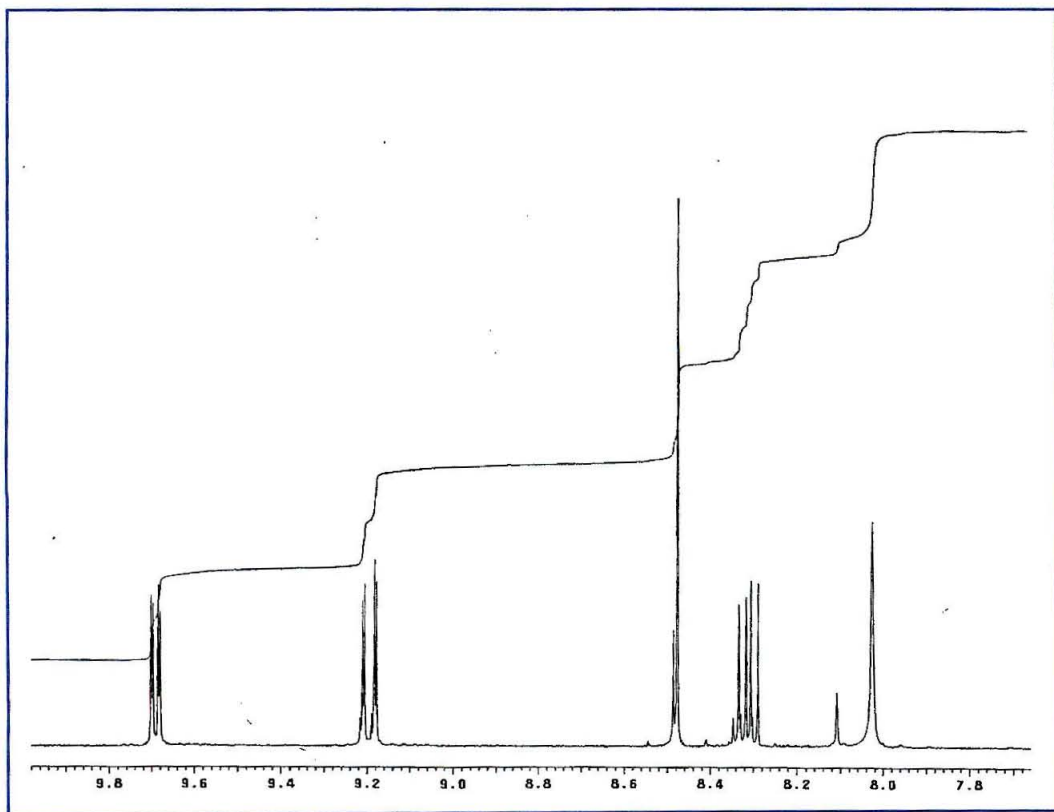


**Figure B.9:**  $^1\text{H}$  NMR of  $(\text{phen})\text{Re}^{\text{I}}(\text{CO})_3(\text{OH}_2)]^{\text{Tf}}$  in  $\text{dmf-d}_3$ .

*References*

- (1) Sullivan, P. B.; Meyer, T. J. *J. Am. Chem. Soc., Chem. Comm.* **1984**, 18, 1244-1245.
- (2) Still, W. C.; Kahn, M.; Mitra, A. *J. Org. Chem.* **1978**, 43, 2923-2925.
- (3) Pearson, D. L.; Tour, J. M. *J. Org. Chem.* **1997**, 62, 1376-1387.
- (4) Springer, D. M.; Wallace, O. B. *Tet. Lett.* **1998**, 39, 2693-2694.